(12) INTERNATIONAL APPLICATION PUBLISHED UNDER THE PATENT COOPERATION TREATY (PCT)

(19) World Intellectual Property Organization
International Bureau

(43) International Publication Date
25 March 2004 (25.03.2004)

PCT

(10) International Publication Number
WO 2004/024191 A2

(51) International Patent Classification[7]: A61K 49/00

(21) International Application Number:
PCT/US2003/028074

(22) International Filing Date:
10 September 2003 (10.09.2003)

(25) Filing Language: English

(26) Publication Language: English

(30) Priority Data:

60/409,850	10 September 2002 (10.09.2002)	US
60/409,851	10 September 2002 (10.09.2002)	US

(71) Applicant *(for all designated States except US)*: **UNIVERSITY OF MARYLAND, BALTIMORE** [US/US]; 520 West Lombard Street, Baltimore, MD 21201-1627 (US).

(72) Inventors; and
(75) Inventors/Applicants *(for US only)*: **LAKOWICZ, Joseph, R.** [US/US]; 10037 Fox Den Road, Ellicott City, MD 21042-2224 (US). **PARFENOV, Alex** [RU/US]; 8 Charles Plaza, Apt. 2302, Baltimore, MD 21201-4235 (US). **GRYCZYNSKI, Ignacy** [PL/US]; 14 Minte Drive, Balltimore, MD 21236-1600 (US). **MALICKA, Johanna, B.** [PL/US]; 1000 Arion Park Road, Apt. 96, Baltimore, MD 21229 (US). **GEDDES, Chris, D.** [GB/US]; 1010 Peppard Drive, Bel Air, MD 21014-6932 (US).

(74) Agents: **WRIGHT, Lee, C.** et al.; Sughrue Mion, PLLC, Suite 800, 2100 Pennsylvania Avenue, NW, Washington, DC 20037-3213 (US).

(81) Designated States *(national)*: AE, AG, AL, AM, AT, AU, AZ, BA, BB, BG, BR, BY, BZ, CA, CH, CN, CO, CR, CU, CZ, DE, DK, DM, DZ, EC, EE, EG, ES, FI, GB, GD, GE, GH, GM, HR, HU, ID, IL, IN, IS, JP, KE, KG, KP, KR, KZ, LC, LK, LR, LS, LT, LU, LV, MA, MD, MG, MK, MN, MW, MX, MZ, NI, NO, NZ, OM, PG, PH, PL, PT,

[Continued on next page]

(54) Title: USE OF METALLIC PARTICLES TO IMPROVE FLUORESCENCE IMAGING

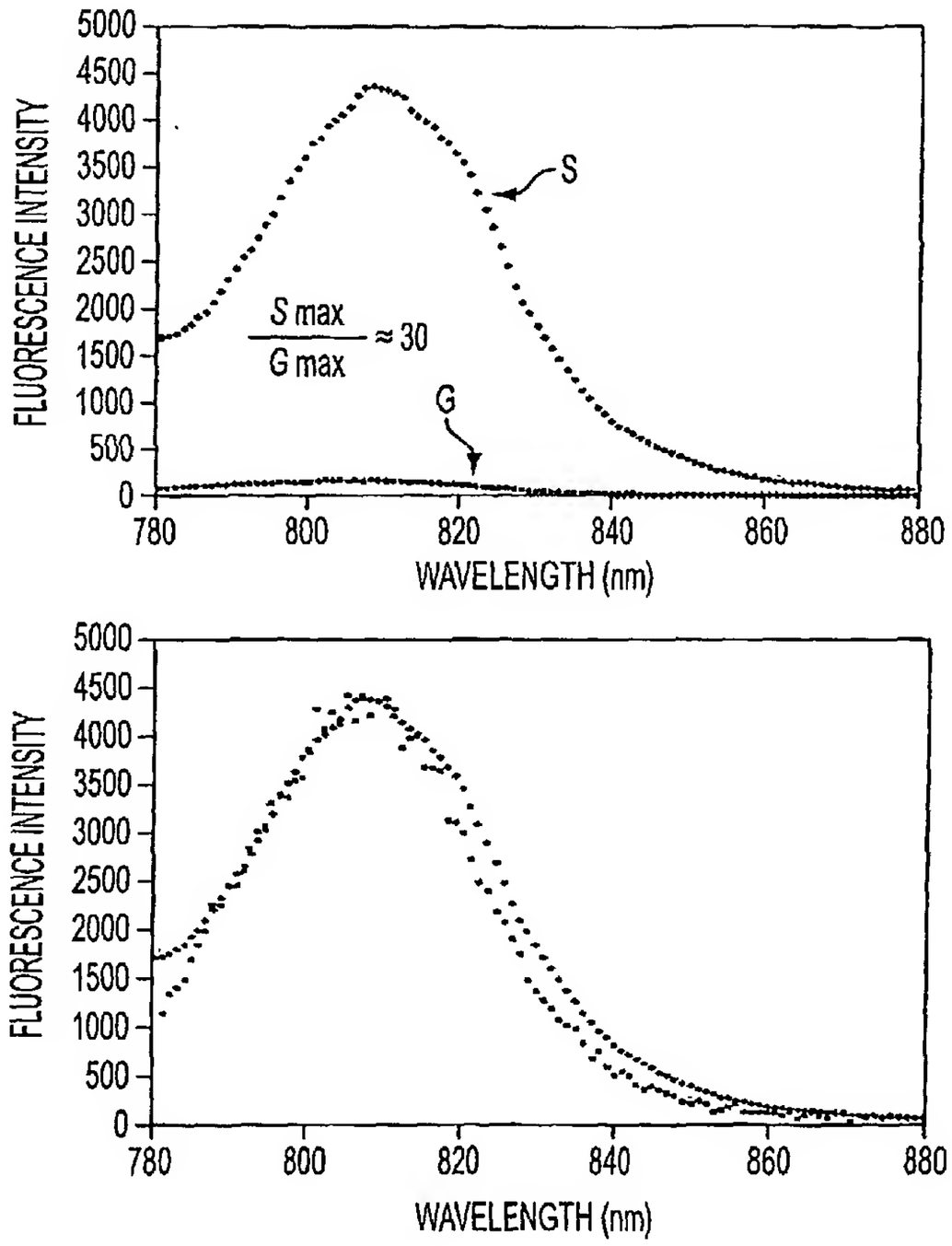

(57) Abstract: A material, metallic colloid or system for enhancing the fluorescence of dye upon exposing the material to irradiation. The material and metal colloid may contain indocyanine dye, albumin and a metallic particle such that the metallic particle provides enhancement of the fluorescence of the indocyanine dye upon exposing said material to irradiation. In the system, the indocyanine dye and the metallic particle are positioned at a distance sufficient to provide an enhancement of the fluorescence of the indocyanine dye upon exposing said system to irradiation. A method of imaging or assaying comprising administering the metallic colloid to a subject and irradiating said subject to detect the presence of indocyanine dye. And the use of metallic surfaces or particles deposited by laser illumination for enhancing the fluorescence a molecule upon exposing the material to irradiation.

WO 2004/024191 A2

RO, RU, SC, SD, SE, SG, SK, SL, SY, TJ, TM, TN, TR, TT, TZ, UA, UG, US, UZ, VC, VN, YU, ZA, ZM, ZW.

(84) **Designated States** *(regional)*: ARIPO patent (GH, GM, KE, LS, MW, MZ, SD, SL, SZ, TZ, UG, ZM, ZW), Eurasian patent (AM, AZ, BY, KG, KZ, MD, RU, TJ, TM), European patent (AT, BE, BG, CH, CY, CZ, DE, DK, EE, ES, FI, FR, GB, GR, HU, IE, IT, LU, MC, NL, PT, RO, SE, SI, SK, TR), OAPI patent (BF, BJ, CF, CG, CI, CM, GA, GN, GQ, GW, ML, MR, NE, SN, TD, TG).

Published:

— *without international search report and to be republished upon receipt of that report*

For two-letter codes and other abbreviations, refer to the "Guidance Notes on Codes and Abbreviations" appearing at the beginning of each regular issue of the PCT Gazette.

USE OF METALLIC PARTICLES TO IMPROVE FLUORESCENCE IMAGING

CROSS REFERENCE TO RELATED APPICATIONS

[01] This application claims benefit of priority of U.S. provisional application number 60/409,851, entitled "USE OF METALLIC COLLOIDS TO IMPROVE FLUORESCENCE IMAGING", filed on September 10, 2002, and benefit of priority of U.S. provisional application number 60/409,850, entitled "ENHANCED FLUORESCENCE BY DEPOSITED METALLIC PARTICLES", filed on September 10, 2002, both of which are incorporated by reference herein in its entirety.

STATEMENT REGARDING FEDERALLY SPONSORED RESEARCH

[02] The work leading to this invention was supported in part by the U.S. Government under grant number RR-08119 awarded by the NIH National Center for Research Resources and under grant number CA-100982 awarded by the National Cancer Institute. Therefore, the U.S. Government may have certain rights in this invention.

BACKGROUND OF THE INVENTION

[03] Indocyanine Green (ICG) is a tricarbocyanine dye with a near infrared absorption and emission maxima near 780 and 820 nm, respectively. The chemical structure of ICG is:

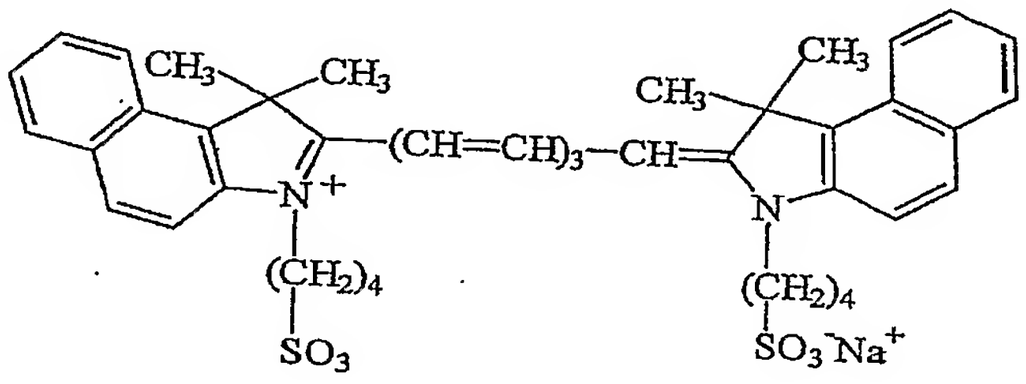

[04] Indocyanine Green is widely used in medical imaging and testing. It has been FDA approved for use in humans, typically by injection. ICG appears to be essentially non-toxic and is rapidly cleared from the body (Henschen et al, Determination of plasma volume and total blood volume using indocyanine green: a short review, *J. Medicine,* 24(1):10-27 (1993) and Ott et al, Hepatic removal of two fractions of indocyanine green after bolus injection in anesthetized pigs, *Am. J. Physiol.*, 266 (*Gastrointest. Liver Physiol.*, 29) (1994)). Indocyanine Green has a large number of medical applications including retinal angiography (Schutt et al, Indocyanine green angiography in the presence of subretinal or intraretinal haemorrhages: clinical and experimental investigations, *Clin. Exper. Investigations*, 30(2):110-114 (2002), Marengo et al, Glaucomatous optic nerve head changes with scanning laser ophthalmoscopy, *Int. Ophthalmology*, 23(4-6):413-423, (2001), Mueller et al, Evaluation of microvascularization pattern visibility in human choroidal melanomas: comparison of confocal fluorescein with indocyanine green angiography, *Graefe's Arch. Clin. Exp. Opthalmol.,* 237:448-456 (1999), Kramer et al, Comparison of fluorescein angiography and indocyanine green angiography for imaging of choroidal neovascularization in hemorrhagic age-related macular degeneration, *Am. J. Opthalmol.*, 129(4):495-500 (2000), Flower, R. W., Experimental studies of indocyanine green dye-enhanced photocoagulation of choroidal neovascularization feeder vessels, *Am. J. Ophalmol.,* 129(4):501-512 (2000), and Flower et al, Theoretical investigation of the role of choriocapillaris blood flow in treatment of subfoveal choroidal neovascularization associated with age-related macular degeneration, *Am. J. Opthalmol,* 132(1):85-93 (2001)), including injecting fluorescence to image the surface vasculature, and using the longer wavelength absorption and emission of ICG to image the choridal vasculature behind the retina (Flower, R. W, *Id.* and Flower et al, *Id.*) measurement of plasma volume (Ishihara et al, Does indocyanine green accurately measure

plasma volume early after cardiac surgery?, *Anesthesia & Analgesia*, 94(4):781-786 (2002)), cardiac output (Sakka et al, Comparison of cardiac output and circulatory blood volumes by transpulmonary thermo-dye dilution and transcutaneous indocyanine green measurement in critically ill patients, *Chest*, 121(2):559-65 (2002)), photocoagulation (Lanzetta, P., ICGA-guided laser photocoagulation of feeder vessels of choroidal neovascular membranes in age-related macular degeneration, *Retina. J. Ret. VIT. Dis.*, 21(5):563-564 (2001)), assessment of burn depth/severity (Still et al, Diagnosis of burn depth using laser-induced indocyanine green fluorescence: a preliminary clinical trial, *Burns*, 27(4):364-371 (2001)), liver function (Silva et al, Changes in susceptibility to acetaminophen-induced liver injury by the organic anion indocyanine green, *Food & Chemical Toxicology*, 39(3):271-278 (2001)), exercise physiology (Boushel et al, Regional blood flow during exercise in humans measured by near-infrared spectroscopy and indocyanine green, J. Appl. Physiol., 89(5):1868-78 (2000)) and guiding of biopsy (Motomura et al, Sentinel node biopsy guided by indocyanine green dye in breast cancer patients, *Japanese J. Clin. Oncol.*, 29(12):604-607 (1999)). ICG is also being investigated for other uses such as optical tomography (Ntziachristos et al, Concurrent MRI and diffuse optical tomography of breast after indocyanine green enhancement, *PNAS*, 97(6):2767-2772 (2000) and Sevick-Muraca et al, Fluorescence and absorption contrast mechanisms for biomedical optical imaging using frequency-domain techniques, *Photochem. Photobiol.*, 66(1):55-64 (1997)) and optical tumor detection (Becker et al, Macromolecular contrast agents for optical imaging of tumors: Comparison of indotricarbocyanine-labeled human serum albumin and transferrin, *Photochem. Photobiol.*, 72(2):234-241 (2000)). In the case of choridal imaging the diagnostic value of ICG could be increased by larger intensities and decreased leakage from the vasculature.

[05] ICG displays complex associative and spectral properties in solution (Devoisselle et al, Fluorescence properties of indocyanine-part 1.: in-vitro study with micelles and liposomes, *SPIE*, 2980-453-460 (1997), Devoisselle et al, Fluorescence properties of indocyanine green / part 2: In vitro study related to *in vivo* behavior, *SPIE*, 2980_293-302 (1997), and Zhou et al, Aggregation and degradation of indocyanine green, *SPIE*, 2128:495-508 (1994)). Its complex spectral behavior and low quantum yield limits some applications. Therefore, there is a need in the art to normalize the spectral properties and improve stability (Rajagopalan et al, Stabilization of the optical tracer agent indocyanine green using noncovalent interactions, *Photochem. Photobiol.*, 71(3):347-350 (2000) and Maarek et al, Fluorescence of indocyanine green in blood: intensity dependence on concentration and stabilization with sodium polyaspartate, *J. Photochem. Photobiol. B : Biology*, 65:157-164 (2001)). These attempts rely on binding ICG to proteins, micelles or membranes, or binding to charged polymers.

[06] DNA sequencing techniques have several disadvantages including high costs resulting from the high cost of the lasers used to excite the fluorescent markers which typically emit in the visible region of light spectrum and the high noise to signal ratio due to the background interferences by biomolecules.

[07] There has also been overwhelming driving forces in analytical, biomedical and materials sciences to fabricate ever faster and smaller devices with enhanced sensitivities, precision and specificity, all with the ultimate goal of engineering devices at both the cellular and molecular level.

[08] The present invention describes a new approach to improving the stability and brightness of dyes used in fluorescence imaging. The present inventors have discovered that improved solubility and spectral properties of dyes may be obtained when the dyes are bound

to albumin to form a conjugate. Further, the present inventors have also discovered that the use of a physical interaction of dyes with metallic silver particles can improve imaging. Preferably the dyes are cyanine dyes. Most preferably, the dyes are ICG.

[09] Metallic particles, such as metallic colloids from a suspension, bind spontaneously to amine-coated surfaces. The present inventors discovered that metallic colloid-coated surfaces increase in the intensity of dyes and particularly ICG, which was held close to the metal surface by adsorbed albumin. The increased intensities of dyes and particularly ICG were also associated with decreased lifetimes and increased photostability, which are indicative of modifying the fluorophores radiative decay rate.

[10] Fluorescence has become the dominant detection technology in medical diagnostics and biotechnology. While fluorescence provides high sensitivity, there exists the need for reduced detection limits and/or small copy-number detection. Detectability is usually limited by autofluorescence of the samples and/or the photostability of the fluorophores. In an effort to obtain increased sensitivity, the use of metallic surfaces or particles to favorably modify the spectral properties of fluorophores has been investigated.

[11] It is possible to prepare metallic surfaces or particles by a variety of methods. For use in medical and biotechnology applications, such as diagnostic or microfluidic devices, it would be useful to obtain metal-enhanced fluorescence (MEF) at precise desired locations in the measurement device.

BRIEF SUMMARY OF THE INVENTION

[12] The use of metal-fluorophore interactions as radiative decay engineering was recently described (Lakowicz, Radiative decay engineering: Biophysical and biomedical applications, *Anal. Biochem.*, 298:1-24 (2001), and Lakowicz et al, Radiative decay engineering 2. Effects of silver island films on fluorescence intensity, lifetimes, and resonance energy/transfer, *Anal. Biochem.* 301:261-277 (2002)). The proximity to the metallic surfaces resulted in increased intensities, decreased lifetimes and moderate increases in photostability. These effects occur because the excited fluorophores interact with freely mobile electrons in the metal, resulting in increased rates of radiative decay.

[13] The metals of the present invention are preferably noble metals. Exemplary metals include, but are not limited to, rhenium, ruthenium, rhodium, palladium, silver, copper, osmium, iridium, platinum, and gold. The most preferable metals are silver and gold. Gold may be avoided because of the absorption of gold at shorter wavelengths. However, gold colloids may be used with longer wavelength red and NIR fluorophores. The metals may be mixtures or alloys of one or more metals. The metal particles can be placed on substrate surfaces as thin films, or deposited on surfaces to form small islands. The surfaces can be metallic or non-metallic. Additionally, the metal particles can be coated with polymers, gels, adhesives, oxides, SiO_2, or biologic material. Exemplary coatings include substances that increase the binding of the metal particle to surfaces or other molecules. The metal particles may be layer(s) of metal formed or coated on non-metal particles. Exemplary substrate surfaces include but are not limited to glass or quartz.

[14] Metal particles or metal films are known and can be produced using known methods. U.S. Appln. No. 10/073,625, which is incorporated by reference in its entirety, discloses examples of preparing metal particles and metal films.

[15] The metal particle may contain a coating to create a separation or a spacer layer to enhance fluorescence. In recent reports the favorable effects of silver particles for increasing the intensities and photostability of fluorophores, particularly those with low quantum yields (Lakowicz, Radiative decay engineering: Biophysical and biomedical applications, *Anal. Biochem.* 298:1-24 (2001), Lakowicz et al, Radiative decay engineering 2. Effects of silver island films on fluorescence intensity, lifetimes, and resonance energy transfer, *Anal. Biochecm.*, 301:261-277 (2002), Lakowicz et al, Intrinsic fluorescence from DNA can be enhanced by metallic particles, *Biochem. Biophys. Res. Commun.*, 286:875-879 (2001), and Gryczynski et al, Multiphoton excitation of fluorescence near metallic particles: Enhanced and localized excitation, *J. Phys. Chem. B.* 106:2191-2195 (2002)). See also Lakowicz, U. S. Patent Application Publication No. US 2002-0160400 A1, published October 31, 2002 (U.S. Patent Appln. No.: 10/073,625), Lakowicz et al, U.S. Patent Application No.:10/426,012, filed April 30, 2003, and Schalkhammer et al, U. S. Patent 5,866,433, issued February 2, 1999, each of which is hereby incorporated by reference herein in their entirety.

[16] Such metallic surfaces interact with the fluorophores by mechanisms that can cause quenching, increased rates of excitation and/or increased quantum yields. These effects were considered theoretically as part of the effort to understand surface enhanced Raman scattering (SERS) (Gersten and Nitzan, Spectroscopic properties of molecules interacting with small dielectric particles, *J. Chem. Phys.*, 75(3):1139-1152 (1981), Weitz and Garoff, The enhancement of Raman scattering, resonance Raman scattering, and fluorescence from molecules absorbed on a rough silver surface, *J. Chem. Phys.*, 78:5324-5338 (1983), and Kummerlen et al, Enhanced dye fluorescence over silver island films: analysis of the distance dependence, *Molec. Phys.*, 80(5):1031-1046 (1993)). For SERS, the most commonly used system are Silver Island Films (SIFs). These films are formed, for example, by chemical

reduction of silver with direct deposition into a glass substrate (Ni and Cotton, Chemical procedure for preparing surface-enhanced Raman scattering active silver films, *Anal. Chem.*, 58:3159-3163 (1986), and Sokolov et al, Enhancement of molecular fluorescence near the surface of colloidal metal films, *Anal. Chem.*, 70:3898-3905 (1998)), resulting in a heterogeneous distribution of silver particles. This process is difficult to control. In contrast, preparation of colloidal suspensions of gold and silver are rather standard and easily controlled to yield a homogeneously sized suspension of spherical metal particles (Turkevich et al, A study of the nucleation and growth processes in the synthesis of colloidal gold, *J. Discuss Faraday Soc.*, 11:55-75 (1951), Henglein and Giersig, Formation of colloidal silver nanoparticles: capping action of citrate, *J. Phys. Chem. B,* 103:9533-9539; and Rivas et al, Growth of silver colloidal particles obtained by citrate reduction to increase the Raman enhancement factor, *Langmuir*, 17:574-577 (2001)), a technology used for hundreds of years for the preparation of colored glasses (Faraday, The Bakerian Lecture. Experimental relations of gold (and other metals) to light, *Philos, Trans.*, 147:145-181 (1957), and Kerker, The optics of colloidal silver: something old and something new, *J. Colloid & Interface Science*, 105(2):297-314 (1985)). Another advantage of a colloidal suspension is that it can be used as an injection for medical imaging.

[17] Numerous publications have appeared on the use of SIFs for SERS (Fleischmann et al, Raman spectra of pyridine adsorbed at a silver electrode, *Chem. Phys. Letts.*, 26(2),163-166 (1974), Chen and Burstein, Giant Raman scattering by molecules at metal-island films, *Phys. Rev. Letts*, 45(15):1287-1291 (1980), Vo-Dinh, Surface-enhanced Raman spectroscopy using metallic nanostructures, *Trends in Anal. Chem*, 17(8-9):557-582 (1998), and Kneipp, et al, Surface-enhanced Raman scattering: A new tool for biomedical spectroscopy, *Current Sci.*, 77(7):915-624 (1999)) and a lesser but significant number of reports of Surface

Enhanced Fluorescence (SEF), which is also known as metal-enhanced fluorescence (MEF), using SIF substrates (Lakowicz, Radiative decay engineering: Biophysical and biomedical applications, *Anal. Biochem.*, 298:1-24 (2001), Lakowicz et al, Radiative decay engineering 2. Effects of silver island films on fluorescence intensity, lifetimes, and resonance energy transfer, *Anal. Biochem.*, 301:261-277 (2002), Lakowicz et al, Intrinsic fluorescence from DNA can be enhanced by metallic particles, *Biochem. Biophys. Res. Commun.*, 286:875-879 (2001), Gryczynski, Multiphoton excitation of fluorescence near metallic particles: Enhanced and localized excitation, *J. Phys. Chem. B*, 106:2191-2195 (2002), Kummerlen et al, Enhanced dye fluorescence over silver island films: analysis of the distance dependence, *Molecular Physics*, 80(5):1031-1046 (1993), Stich et al, DNA biochips based on surface-enhanced fluorescence (SEF) for high-throughput interaction studies, *SPIE*, 4434:128-137 (2001), and Schalkhammer et al, Detection of fluorophore-labeled antibodies by surface-enhanced fluorescence on metal nanoislands, *SPIE*, 2976:129-136 (1997)). In contrast, fewer publications exist on SERS using silver colloids and only a very few reports of SEF using colloids (Marchi et al, Photophysics of rhodamine B interacting with silver spheroids, *J. Colloid & Interface Science*, 218:112-117 (1999), and Sokolov et al, Enhancement of molecular fluorescence near the surface of colloidal metal films, *Anal. Chem.*, 70(18):3898-3905 (1988)). These reports describe fluorophores with visible excitation and emission wavelengths. The results have been contradictory. Since the fluorophores interact with the metal through the surface plasmon resonance, which for silver the adsorption maximum is near 430 nm, Applicants did not know if silver colloids would enhance the emission of ICG with absorption and emission maxima of 795 and ≈810 nm, respectively. Additionally, significantly larger effects on fluorescence are predicted for elongated silver particles than for spheres (Gersten and Nitzan, Spectroscopic properties of molecules interacting with small

dielectric particles, *J. Chem. Phys.*, 75(3):1139-1152 (1981)) and thus it was not clear if significant enhancements could be observed using spherical colloids.

[18] In the present invention, Applicants studied ICG bound to albumin, such as human serum albumin (HSA), bovine albumin, ovalbumin, and etc.

[19] ICG bound to HSA is the dominant form of ICG following intravenous injection. Additionally, ICG bound to HSA further bound to metal or non-metal surfaces was studied. The metal surfaces may be a silver island film (SIF), which is a non-continuous coating of silver particles on a glass substrate. The silver may be deposited by, for example, chemical reduction of silver (Ni, Chemical procedure for preparing surface-enhanced Raman scattering active silver films, Anal. Chem., 58:3159-2163 (1986)), or deposition by laser illumination as discussed below. The quartz and quartz-SIF surfaces were coated with HSA, which is known to passively adsorb to such surfaces (Sokolov et al, Enhancement of molecular fluorescence near the surface of colloidal metal films, Anal. Chem., 70:3898-3905 (1998)), and the fluorescent spectral properties of non-covalent ICG-HSA complexes in the absence and presence of the silver particles determined.

[20] Additionally, albumin proteins are known to spontaneously bind to glass and silver surfaces forming essentially a complete monolayer (Sokolov, Enhancement of molecular fluorescence near the surface of colloidal metal films, *Anal. Chem.*, 70(18):3898-3905 (1998)). Metal colloids, such as silver and gold colloids, are known to bind spontaneously to surfaces coated with compounds containing an amino group (Sokolov et al, Enhancement of molecular fluorescence near the surface of colloidal metal films, *Anal. Chem.*, 70(18):3898-3905 (1998), and Grabar et al, Preparation and characterization of Au colloid monolayers, *Anal. Chem.*, 67:735-743 (1995)). An example of an compounds containing an amino group is 3-Aminopropyltrimethoxysilane (APS).

[21] This interaction was used to bind silver colloids to microscope slides covered with amino groups, which in turn were coated with ICG-HSA complexes. This approach makes it easy to wash away unbound colloids and proteins. Additionally, the use of colloids on surfaces circumvented problems of low particle concentration of a colloid suspension with a reasonable optical density of ≈ 0.3. The amine groups can be used to control spacing and the location of the metallic colloids.

[22] The versatility of the present invention can be useful in the many envisaged analytical applications of metal-enhanced fluorescence, such as disposable sensors, gene chips or microfluidic type and lab-on-a-chip based sensing (Christodoulides et al, A microchip-based multianalyte assay system for the assessment of cardiac risk, Anal. Chem., 74:3030-3036 (2002), Verpoorte, Microfluidic chips for clinical and forensic analysis, Electrophoresis, 23:677-712 (2002) and Keir et al, SERRS. In Situ substrate formation and improved detection using microfluidics, Anal. Chem., 74(7): 1503-1508 (2002)).

[23] The present invention also relates to metallic surfaces or particles deposited by laser illumination. Metallic surfaces or particles deposited by laser illumination results in an increased intensity of a fluorescent probe. For example, with silver as the metal particle and locally bound indocyanine green as the fluorescent probe, a ~7-fold increased intensity of locally bound indocyanine green is achieved. The increased intensity is accompanied by a decreased lifetime and increased photostability. The use of enhanced fluorescence with light-deposited silver extends the range of applications of metal-enhanced fluorescence. The use of metallic surfaces or particles deposited by laser illumination in the disclosures of Lakowicz, U. S. Patent Application Publication No. US 2002-0160400 A1, published October 31, 2002 (U.S. Patent Appln. No.: 10/073,625), Lakowicz et al, U.S. Patent Application No.:10/426,012, filed April 30, 2003, and Schalkhammer et al, U. S. Patent

5,866,433, issued February 2, 1999, is specifically contemplated (each of which is incorporated by reference above).

[24] The light-directed deposition of silver is widely applicable. The metallic surfaces or particles deposited by laser illumination may be used in the photolithographic preparation of surfaces for enhanced fluorescence in microfluidics, medical diagnostics and other applications.

[25] In recent years a number of laboratories have reported light-induced reduction of silver salts to metallic silver (Bell and Myrick, Preparation and characterization of nanoscale silver colloids by two novel synthetic routes, J. Colloid and Interface Sci., 242:300-305 (2001), Rodriguez-Gattornoet al, Metallic nanoparticles from spontaneous reduction of silver(I) in DMSO. Interaction between nitric oxide and silver nanoparticles, J. Phys. Chem. B., 106:2482-2487 (2002), Abid et al, Preparation of silver nanoparticles in solution from a silver salt by laser irradiation, Chem. Communications, 7:792-793 (2002) and Pastoriza-Santos et al, Self-assembly of silver particle monolayers on glass from Ag+ solutions in DMF, J. Colloid and Interface Science, 221:236-241 (2000)). Typically a solution of silver nitrate is used which contains a mild potential reducing agent such as a surfactant (Abid et al, Id.) or dimethylformamide (Pastoriza-Santos et al, Id.). Exposure of such solutions to ambient or laser light typically results in the formation of silver colloids in suspension or on the glass surfaces.

[26] Applicants recently reported increased intensities of ICG-HSA when bound to silver island films (SIFs) (Malicka et al, Metal-enhanced emission from indocyanine green: A new approach to in-vivo imaging, Journal of Biomedical Optics (submitted July, 2002). These films are formed by chemical reduction of silver and consist of a heterogeneous population of silver particles bound to glass (Ni and Cotton Chemical procedure for preparing surface-

enhanced Raman scattering active silver films, Anal. Chem., 58:3159-3163 (1986). SIFs are frequently used for SERS. To the best of Applicants' knowledge, there have been no reports of SERS or SEF using light-deposited silver.

BRIEF DESCRIPTION OF THE DRAWINGS

Figure 1: Sample geometry (top), AFM image (bottom left) and absorption spectrum (bottom right).

Figure 2. Emission spectra of indocyanine green-albumin (ICG-HSA) bound to unsilvered quartz slides or silver island films. Top panels, as measured; bottom panel, peak normalized.

Figure 3. Time-dependent intensity decays of ICG-HSA, top: time-domain data, bottom: frequency-domain data for ICG-HSA on silver.

Figure 4. Impulse response functions of ICG-HSA 1) in buffer, 2) Quartz and 3) On silver island films, i.e. the α's and τ's from Table 1, which were obtained from the convolution procedure.

Figure 5. Intensity decay of ICG-HSA with time-integrated areas normalized to the relative steady state intensities (Figure 2).

Figure 6. Photostability of ICG-HSA on quartz and on SIFs, measured with the same excitation power (top) and with adjusted power to provide the same initial fluorescence intensity (bottom).

Figure 7. Emission spectra of ICG in blood.

Figure 8. Photostability of ICG in blood (top) and emission spectra before and after photostability test on silver (bottom).

Figure 9. A) Glass surface geometry. 3-Aminopropyltrimethoxysilane (APS) is used to functionalize the surface of the glass with amine groups which readily bind silver colloids. B) The sample geometry.

Figure 10. Experimental geometry.

Figure 11. Top: Absorption of silver colloids immobilized on APS coated glass.

Bottom: AFM image of a silver colloid coated, 0.5% v/v APS coated glass slide.

Figure 12. Top: Fluorescence intensity of HSA-ICG coated glass, G, and above silver colloids, S, Ex = 760 nm, Em = 810 ± nm.

Bottom: Fluorescence intensities normalized to the intensity on silver colloids.

Figure 13. Fluorescence intensity of HSA-ICG on silver colloids as a function of increased [APS] used. Cleaned glass slides were initially soaked in: a - 0.1; b - 0.25; c - 0.5; d - 1.0 and e - 1.25% (v/v) APS solution for 4 hrs, washed and soaked in colloid solution for 4 days. G - Fluorescence intensity of HSA-ICG deposited on 0.5 % APS covered glass.

Figure 14. Top: Complex intensity decays of ICG-HSA in a cuvette (buffer) (C), on glass slides (G), and silver colloids on APS treated glass slides (S). RF - Instrumental response function.

Bottom: Data from convolution process normalized to steady state intensity, i.e. area under S = 39.5 *area under G, c.f. Figure 13.

Figure 15. Emission spectrum (magic angle conditions) of ICG-HSA on silver colloids, scanning through the excitation wavelength, (vertically polarized 760 nm), using the emission filters used to collect the TD data (i.e. red long-pass filter and a 830 ± 10 nm interference filter).

Figure 16. Top – Photostability of ICG-HSA on glass and silver colloids, measured using the same excitation power at 760 nm and (bottom) with power adjusted to give the same initial fluorescence intensities. In all measurements vertically polarized excitation was used, while fluorescence emission was observed at the magic angle, i.e. 54.7°.

Figure 17. Experimental set-up for laser deposition of silver on APS-coated glass microscope slides.

Figure 18. Absorption spectrum of a 0.5 % v/v APS-coated glass slide after 5 mins. illumination with a 442 nm HeCd laser.

Figure 19. Top - Fluorescence intensity of HSA-ICG coated glass, I_G and laser deposited silver, I_S (442 nm, 15 mins. exposure).

Bottom - Fluorescence intensities normalized to the intensity on silver.

Figure 20. Time-dependent intensity decays of ICG-HSA in solution (buffer), bound to glass, and on laser-deposited, LD, silver. RF- Instrumental Response function < 40 ps fwhm.

Figure 21. Top - Photostability of ICG-HSA on glass, G, and laser deposited silver, S, measured with the same excitation power at 760 nm.

Bottom - with the laser power at 760 nm adjusted for the same initial fluorescence intensity. Laser deposited samples were made by focusing 442 nm laser light onto APS-coated glass slides immersed in a $AgNO_3$, citrate solution for 15 mins. The OD of the sample was ca. 0.3.

Figure 22. Top - Inverted Axiovert 135 TV microscope with epi-illumination for LD.

Bottom - Image of silver spots, produced by LD, using transmitted light illumination. The diameter of a spot is typically 50 μm. The irradiance was 560 W/cm^2 with a 40 x objective NA 1.2. Images A-F were taken 5 seconds apart.

DETAILED DESCRIPTION OF THE INVENTION

[27] The intensity decay data were analyzed in terms of the multi-exponential model

$$I(t) = \sum_i \alpha_i \exp(-t/\tau_i) \qquad (1)$$

where α_i are the amplitudes, τ_i are the decay times and $\Sigma \alpha_i = 1.0$. The contribution of each component to the steady state intensity is given by

$$f_i = \frac{\alpha_i \tau_i}{\sum_j \alpha_j \tau_j} \qquad (2).$$

[28] The mean decay time is given by

$$\bar{\tau} = \sum_i f_i \tau_i \qquad (3).$$

[29] The amplitude-weighted lifetime is given by

$$<\tau> = \sum_i \alpha_i \tau_i \qquad (4).$$

[30] The value of α_i and τ_i were determined by non-linear least squares using non-linear least squares impulse reconvolution with a goodness-of-fit χ_R^2 criterion.

[31] Fluorophores can have several interactions with metallic surfaces, including quenching, an increase in the rate of radiative decay, or an increased rate of excitation due to increased excitation field. This last interaction is called the "lightening rod effect". Lifetime measurements can distinguish between these interactions. The intensity will be higher due to the increased electric field around the metal particles (Kummerlen et al, Enhanced dye fluorescence over silver island films: analysis of the distance dependence, *Molec. Phys.*,

80(5):1031-1046 (1993)). Consider the usual definition the lifetime (τ) and quantum yield (Q)

$$Q = \frac{\Gamma}{\Gamma + k_{nr}} \quad (5)$$

$$\tau = \frac{1}{\Gamma + k_{nr}} \quad (6)$$

where Γ is the radiative decay rate and k_{nr} is the sum of the non-radiative decay rates. A quenching interaction will increase k_{nr} so that the quantum yields and lifetimes decrease in unison. An increased rate of excitation due to the lightening rod effect will not affect Γ or k_{nr}.

[32] Unusual effects are expected if the radiative decay rate is increased from Γ to $\Gamma + \Gamma_m$ near the metal. Then the quantum yield and lifetimes are given by

$$Q = \frac{\Gamma + \Gamma_m}{\Gamma + \Gamma_m + k_{nr}} \quad (7)$$

$$\tau = \frac{1}{\Gamma + \Gamma_m + k_{nr}} \quad (8)$$

[33] An increase in the total radiative rate to $\Gamma + \Gamma_m$ results in an increased quantum yield and a decreased lifetime.

[34] Additional insight can be gained by examining the intensity decays normalized so that the integrated area under the decay is equal to the relative steady state intensities. This normalization is based on the fact that the time-integrated intensity decay, given by the $\sum \alpha_i \ \tau_i$ products, is proportional to the steady state intensity.

Multi-Exponential Intensity Decays

[35] The intensity decays of fluorophores near metallic particle display unique features not encountered in typical multi-exponential decays. This difference can be seen by a close examination of the decay parameters with careful definition of the parameters. First consider a fluorophore which displays a single exponential decay:

$$I(t) = k \Gamma N(t) = k \Gamma N_0 \exp(-t/\tau).$$

[36] In this expression k is an instrumental constant, Γ is the radiative decay rate, N(t) is the time-dependent excited state population, N_0 is the excited state population at time = 0 and τ is the lifetime. The steady state intensity is given by the integral of I(t) over all times:

$$I = \int_0^\infty I(t)\, dt = k \Gamma \tau N_0.$$

From equations 5 and 6 we see that $\Gamma \tau = Q$ the quantum yield so that the steady state intensity is given by

$$I = k Q N_0.$$

[37] Now assume that the fluorophore is in two environments, 1 and 2, which display different lifetimes. The total (T) intensity observed from these two populations is given by

$$I_T(t) = k N_0 \left[n_1 \Gamma \exp(-t/\tau_1) + (1 - n_1), \Gamma \exp(-t/\tau_2)\right].$$

where n_1 and $n_2 = 1 - n_1$ are the fractional populations in each environment. This expression contains a valid but often forgotten assumption that the radiative decay rate of the fluorophore is the same in both environments. This is a good assumption for an intensity

decay due to a single fluorophore because the radiative decay rate is determined by the extinction coefficient which is not significantly sensitive to the local environment. For simplicity, we are neglecting any difference in the local refractive index surrounding the fluorophore.

[38] Eq. A5 can demonstrate that the pre-exponential factors in an intensity decay for a fluorophore in two environments, both without metals, represent the molecular fractions. A measured intensity decay is represented by

$$I_T(t) = \alpha_i \exp(-t/\tau_1) + \alpha_2 \exp(-t/\tau_2)$$

where $\alpha_1 + \alpha_2$ is typically normalized to unity. Comparison of eqs. A5 and A6 yield the unnormalized α_1 and α_2 values as

$$\alpha_1 = k N_0 \Gamma n_1$$

$$\alpha_2 = k N_0 \Gamma (1 - n_1) = k N_0 \Gamma n_2 .$$

The normalized values of α_1 and α_2 can be obtained by dividing each by the sum

$$\alpha_1 + \alpha_2 = k N_0 \Gamma .$$

This yields

$$\alpha_1 = n_1$$

which demonstrates that the α_i values represent the molecular fractions.

[39] The total steady state intensities can be calculated using Eq. A2 yielding

$$I_T = k N_0 [n_1 Q_1 + n_2 Q_2] .$$

The fractional intensities from each environment are given by

$$f_1 = \frac{n_1 Q_1}{n, Q_1 + n_2 Q_2}$$

$$f_2 = \frac{n_2 \; Q_2}{n_1 \; Q_1 \; t \, n_2 \; Q_2}.$$

This result shows that the fractional steady state intensities do not represent the fraction of fluorophores in each environment.

[40] This description of a multi-exponential decay may seem simple. However, this detailed description is needed to show the different meaning of the α_i and f_i values with metal-enhanced fluorescence.

INTENSITY DECAYS WITH METAL-ENHANCED FLUORESCENCE

[41] Assuming there is a single fluorophore which displays a single exponential decay in the absence of metal (τ) and when near a metal (τ_m) and also assuming that the metal causes an increase of the radiative decay rate from Γ in the absence of metal to Γ_m when near the metal, the total intensity decay is then given by

$$I_T \; (t) = k \; N_0 \; [(1 - m) \; \Gamma \exp(-t/\tau) + m \; \Gamma \exp(-t/\tau_m)]$$

where 1 - m and m are the fractional populations distant from and near the metal, respectively. The normalized pre-exponential factors are thus given by

$$\alpha = \frac{(1 - m) \; \Gamma}{(1 - m) \; \Gamma + m \; \Gamma_m}$$

$$\alpha_m = \frac{m \; \Gamma_m}{(1 - m) \; \Gamma + m \; \Gamma_m}$$

In contrast to eqs. A9 and A10 the α_i values do not represent the molecular fractions. The change in radiative decay rate results in α_i values which are weighted by the Γ_i values. This

explains values of α_i summarized in Table 1. Since only a fraction of the ICG is bound to silver islands, and this fraction is probably near 25%, one does not expect that α_i value for the short component to be larger than 0.25. However, the value for ICG-HSA on the SIF is 0.982. We believe this result is due to an increased radiative decay rate of ICG near silver, and the weighed α_m value shown in eq. A16.

[42] Eqs. A2 and A14 can be used to calculate the total steady state intensity

$$I_T = (1 - m) \Gamma \tau + m \Gamma_m \tau_m$$

$$I_T = (1 - m) Q + m Q_m .$$

Prior to normalization the value of I_T is proportional to the sum of the $\alpha_i \tau_i$ products, in this case m and 1 - m. For this reason we feel it is preferable to use $<\tau>$ (eq. 4) rather than $\bar{\tau}$ (Eq. 3) when comparing the changes in intensity and lifetime on quartz and near SIFs.

ICG Bound to HAS

MATERIALS AND METHODS

[01] ICG was obtained from Sigma. ICG bound to HSA was prepared by mixing an aqueous solution of ICG with a solution of HSA to a final concentration of 30 μM ICG and 60 μM HSA. Immediately upon mixing the absorption spectrum of ICG changed from the aggregate spectra with two absorption maxima near 700 nm and 780 nm to the monomer spectrum with an absorption maximum near 795 nm. Concentrations were determined using ε(780 nm) = 130,000 M^{-1} cm^{-1} for ICG and ε(278 nm) = 37000 M^{-1} cm^{-1} for HSA. Binding to the surface was accomplished by soaking both the quartz and the SIF slides in the ICG-HSA solution for overnight, followed by rinsing with water.

SILVER ISLAND FILMS

[44] Silver island films were formed on quartz microscope slides according to published procedures (Ni and Cotton, Chemical procedure for preparing surface-enhanced Raman

scattering active silver films, *Anal. Chem.*, 58:3159-3163 (1986)), as modified in recent reports (Lakowicz, Radiative decay engineering: Biophysical and biomedical applications, *Anal. Biochem.*, 298:1-24 (2001)). This procedure consists of reducing silver nitrate with D-glucose under controlled conditions (Lakowicz, Radiative decay engineering: Biophysical and biomedical applications, *Anal. Biochem.*, 298:1-24 (2001)). This procedure results in a partial coating of the quartz with silver islands (Figure 1, bottom left). The diameters of the islands are from 100 to 500 nm across and near 60 nm high, with some aggregates. These particles display a characteristic surface plasmon resonance with a maximum near 480 nm characteristic of silver particles, with an optical density near 0.2 (Figure 1, bottom right).

SAMPLE GEOMETRY

[45] Our sample configuration is shown in Figure 1, top. Half of the slide was covered with SIFs. The albumin-coated surface, with and without SIFs, was covered with the other side of a demountable cuvette, with water between the surfaces.

FLUORESCENCE MEASUREMENTS

[46] Emission spectra were obtained using a Spectra Physics Tsunami Ti:Sapphire laser in the CW (non-pulsed) mode with output at 765 nm. The emission spectra were recorded through a long pass filter from Edmund Scientific which cut off wavelengths below 780 nm. Intensity decays were measured in the time-domain using 750 nm excitation from a mode-locked Argon-ion pump, cavity dumped Pyridine 2 dye laser with a 3.77 MHz repetition rate. Time-correlated single photon counting was accomplished using a SPC630 PC Card from Beckor & Hichl GmbH, in reverse start-stop mode, and a microchannel plate PMT. The instrumental response function, determined with the sample geometry (Figure 1) and a scattering sample was typically < 30 ps fwhm. Data analysis was performed using non-linear least squares impulse reconvolution with a goodness of fit, χ_R^2, criterion. For lifetime

measurements, a long pass filter with an additional 830 nm interference filter to alleviate scattered light was used. All measurements were performed using front-face geometry in a 0.1 mm demountable cuvette or between quartz slides, with vertically polarized excitation and fluorescence emission observed at the magic angle, 54.7°. (The magic angle is the preferable observation angle. Any angle may be used, preferably, within from 50 to 60°.) Frequency-domain measurements (Laczko et al, A 10-Ghz frequency-domain fluorometer, *Rev. Sci. Instrum.*, 61:2331-2337 (1990)) were performed using 700 nm excitation, 7 ps pulses at 7.6 MHz, from a Pyridine 1 dye laser. This instrument has an upper frequency limit of 10 GHz and is capable of measuring decay times of just several ps. In the results discussed below, the intensity decay data were analyzed using the equations set forth above.

RESULTS

[47] Emission spectra of ICG-HSA bound to quartz or SIFs are shown in Figure 2. The intensity of ICG is increased approximately 20-fold on the SIFs as compared to the unsilvered quartz surface (top). The emission spectrum was not detectably shifted by the silver particles (bottom). The same increase in ICG emission whether the surfaces were coated with HSA, which already contained bound ICG, or if the surfaces were first coated with HSA followed by exposure to a dilute aqueous solution of ICG was found. From ongoing studies of albumin-coated surfaces, we know that roughly the same amount of HSA binds to each surface, with the difference in binding being less than a factor of two (Malicka et al, Effects of fluorophore-to-silver distance on the emission of cyanine-dye labeled oligonucleotides, *Anal. Biochem.* (2002)). Hence the intensity increase seen on the SIF is not due to increased ICG-HSA binding but rather is due to a change in the quantum yield and/or rate of excitation of ICG near the silver particles.

[48] The intensity decay of ICG-HSA on quartz or SIFs (Figure 3, top) was examined. The intensity decays much more rapidly when bound to the SIF as compared to the quartz surface. When bound to SIFs the intensity decay of ICG-HSA becomes dominated by a short decay time near 6 ps. Because of the rapid decay components seen in the time-domain data, the intensity decays with our 10 GHz frequency-domain instrument was examined (Laczko et al, A 10-Ghz frequency-domain fluorometer, *Rev. Sci. Instrum.*, 61:2331-2337 (1990)). These measurements also show a dominant 6 ps component (Figure 3, bottom). The similarity of the intensity decays measured in the time and frequency-domain can be seen from the impulse response functions (Figure 4). These functions also clarify the visual difference between the cuvette and on quartz as due to the effects of convolution of the impulse response function with the instrument response function. This component is attributed to a population of ICG molecules which are an appropriate distance from a silver surface to display an increased quantum yield and decreased lifetime. In recent studies the maximum enhancement was observed for fluorophores 40-90 Å from the silver surfaces (Lancaster and Stead, Silver acetate for smoking cessation, *Cochrane Database System Review,* 2:CD000191 (2000)).

[49] The data obtained is shown in Table 1 below.

Table 1. Multi-exponential intensity decay of ICG-HSA.

Sample[a]	α_i	τ_i (ns)	f_i	$\bar{\tau}$ (ns)	<τ>(ns)	χ_R^2
In water, TD[a]	0.158	0.190	0.05	-	-	
	0.842	0.615	0.95	0.592	0.548	1.4
On quartz	0.558	0.233	0.272	-	-	
	0.442	0.792	0.728	0.645	0.484	1.4
On SIFs, TD[a]	0.993	0.006	0.705	-	-	
	0.005	0.215	0.127	-	-	
	0.002	0.799	0.168	0.151	0.008	1.4
On SIFs, FD[b]	0.982	0.006	0.756	-	-	
	0.016	0.067	0.130	-	-	
	0.001	0.752	0.114	0.099	0.008	1.8

[a] Time-domain

[b] Frequency-domain

[50] Examination of Table 1 reveals that the pre-exponential factor for the shortest decay time, presumably for ICG-HSA on SIFs, is 0.982. It is well known that for a fluorophore in two environments, with a different lifetime in each environment, the normalized α_i values represent the fraction of molecules present in each environment. This comparison gives the erroneous impression that 98% of the ICG-HSA molecules display enhanced fluorescence. However, the α_i values only represent the molecular fractions when the radiative decay rate is the same in each environment or for each lifetime component. If the radiative decay rate of a population is increased, as we believe occurs near SIFs, then the normalized α_i value for this population is larger than the molecular fraction near the SIFs. See the formulae above.

[51] Examining the intensity decays normalized so that the integrated area under the decay is equal to the relative steady state intensities as discussed above, Figure 5 shows that the 6 ps component is a new component which appears without a significant decrease in the long lived component. This result suggests that the 6 ps component is due to a small subpopulation of the ICG-HSA molecules, which are at a distance from the metal which results in dramatically increased fluorescence. The signal from ICG could be enhanced to a greater extent using procedures which position a larger fraction of the ICG molecules near the silver surfaces.

[52] ICG is known to rapidly degrade in solution due to chemical and/or photochemical processes. The 20-fold increase in intensity of ICG-HSA seen in Figure 2 would not be useful if the sample degraded 20-fold more rapidly. The steady state intensity of ICG-HSA with continuous illumination was examined. Upon initial exposure the relative intensity of ICG-HSA decays more rapidly on SIFs than on quartz without SIFs (Figure 6, top). However, the effect is modest and the photobleaching rates become comparable after one minute. If the illumination intensity is adjusted to yield the same intensity at the start of illumination this ICG-HSA on SIFs photobleaches somewhat slower (Figure 6, bottom). The detectable signal from the ICG-HSA is given by the area under these photobleaching curves, demonstrating that, prior to photobleaching, about 20-fold more emission can be obtained on SIFs than on quartz without SIFs. This increased signal may be larger if the measurements were intended to longer times. Importantly, the ICG intensity near SIFs remain higher even after the initial decrease in intensity (Figure 6, top). Thus, ICG will display higher intensities for longer times when bound near silver particles.

DISCUSSION

[53] For purposes of injection for *in vivo* medical applications, the use of colloidal suspensions of the metal is preferable rather than SIFs. It appears that colloidal silver is

deemed safe because it has been used for topical applications, as an antibiotic and ingested orally to aid in cessation of smoking (Lancaster and Stead, Silver acetate for smoking cessation, *Cochrane Database System Review*, 2:CD000191 (2000), Hymowitz and Eckholdt, Effects of a 2.5 mg silver acetate lozenge on initial and long-term smoking cessation, *Preventive Medicine*, 25(5):537-46 (2000)). Sublingual applications of colloidal silver results in rapid transport into the bloodstream (Bromberg et al, Sustained release of silver from periodontal wafers for treatment of periodontitis, *J. Controlled Release*, (68(1):63-72 (2000)). Gold is used as an injectable suspension for treatment of arthritis (Wright, Oral gold for rheumatoid arthritis, *British Med. J. Clin. Res. Ed.*, 289(6449):858-9 (1984)). While particulates may seem unsuitable for injection, there are many ongoing studies on using polymeric particles to deliver protein and drugs (Wang and Wu, Preparation and characterization of agarose hydrogel nanoparticles for protein and peptide drug delivery, *Pharmaceutical Dev. & Technol.*, 2(2):135-142 (1997), Hood et al, Tumor regression by targeted gene delivery to the neovasculature, *Science*, 296:2402-eoa (2002)), or MRI contrast agents (Adzamli et al, Preliminary evaluation of a polyethyleneglycol-stabilized manganese-substituted hydroxylapatite as an intravascular contrast agent for MR angiography, *J. Magnetic Resonance Imaging*, 7(1):204-208 (1997), Josephson et al, A functionalized superparamagnetic iron oxide colloid as a receptor directed MR contrast agent, *Magnetic Resonance Imaging*, 8:637-646 (1990)). No literature was found describing the use and/or toxicity of injected silver colloids.

[54] Another preferred embodiment is the combined use of enhanced fluorescence and the scattering properties of metallic colloids. The surface plasmon of colloidal silver, gold and some other metals results in high cross sections for light scattering (Yguerabide and Yguerabide, Light-scattering submicroscopic particles as highly fluorescent analogs and their

use as tracer labels in clinical and biological applications - I. Theory, *Anal. Biochem.*, 262:137-156 (1998), Yguerabide and Yguerabide, Light-scattering submicroscopic particles as highly fluorescent analogs and their use as tracer labels in clinical and biological applications - II. Experimental characterization, *Anal. Biochem.*, 262:157-176 (1998)). The strong scattering makes it easy to detect low concentrations of particles (Schultz et al, Single-target molecule detection with nonbleaching multicolor optical immunolables, *PNAS*, 97(3):996-1001 (2000)). Both the strong scattering and enhanced fluorescence can be used for improved detection in tissues. Alternatively, the metal colloids may be derivatized with sensing fluorophores, such as those sensitive to pH or anions or cations. In this case the scattering can be used to locate the colloids, and the fluorophore emission used to determine the local concentration of analytes.

AMINE

MATERIALS AND METHODS

[55] ICG and HSA were obtained from Sigma and used without further purification. Concentrations of ICG and HSA were determined using extinction coefficients of ε (780 nm) = 130,000 M^{-1} cm^{-1} and ε (278) nm = 37,000 M^{-1} cm^{-1}, respectively.

[56] Glass microscope slides were cleaned by immersion in 30% v/v H_2O_2 and 70% v/v H_2SO_4 for 48 hrs and then washed in distilled H_2O. The glass surfaces were coated with amino groups by soaking the slides in a solution of 3-aminopropyltrimethoxysilane (APS) with different percentages APS (v/v), and different immersion times as indicated.

[57] Silver colloids were formed by the reduction of a warmed solution of silver nitrate and sodium citrate. This procedure is reported to yield homogeneously sized colloids near 20-30 nm in diameter (Turkevich et al, A study of the nucleation and growth processes in the synthesis of colloidal gold, *J. Discuss Faraday Soc.*, 11:55-75 (1951), Henglein and Giersig,

Formation of colloidal silver nanoparticles: capping action of citrate, *J. Phys. Chem. B*, 103:9533-9539; Rivas et al, Growth of silver colloidal particles obtained by citrate reduction to increase the Raman enhancement factor, *Langmuir*, 17:574-577 (2001)). The APS treated slides were soaked in the colloid suspension for the times indicated in the text, followed by rinsing with distilled water. Binding the ICG-HSA to the surfaces, whether quartz or silver, was accomplished by soaking both the quartz and colloid coated slides in a 30 μM ICG, 60 μM HSA solution overnight, followed by rinsing with water to remove the unbound material.

[58] The glass or colloid surfaces were examined in a sandwich configuration in which two coated surfaces faced inwards toward an approximate 1 μm thick aqueous sample (Figure 9). In each case the slides were fully coated with APS but only half coated with silver colloids. Excitation and observation were by the front-face configuration (Figure 10). Steady-state emission spectra were recorded using a SLM 8000 spectrofluorometer with excitation using a Spectra Physics Tsunami Ti:Sapphire laser in the CW (non-pulsed) mode with ≈200 mW 760 nm output.

[59] Time-resolved intensity decays were measured using reverse start-stop time-correlated single photon counting (TCSPC). Vertically polarized excitation at ≈760 nm was obtained using a mode-locked argon-ion pump, cavity dumped Pyridine 2 dye laser with a 3.77 MHz repetition rate. The instrument response function, determined using the experimental geometry in Figure 10, for silver colloid films, was typically <50 ps fwhm. The emission was selected at the magic angle, 54.7°, using a long-pass filter (Edmund Scientific) which cut off wavelengths below 780 nm, with an additional 830 ± 10 nm interference filter. Control measurements with colloid-coated surfaces without ICG-HSA showed that scattered light contributed less than 1 % to the signal of ICG-HSA with or without colloids, which is an important control given the high scattering cross section of metal colloids (Yguerabide and

Yguerabide, Light-scattering submicroscopic particles as highly fluorescent analogs and their use as tracer labels in clinical and biological applications - I. Theory, *Anal. Biochem.*, 262:137-156 (1998), Yguerabide and Yguerabide, Light-scattering submicroscopic particles as highly fluorescent analogs and their use as tracer labels in clinical and biological applications - II. Experimental characterization, *Anal. Biochem.*, 262:157-176 (1998) and Schultz et al, Single-target molecule detection with nonbleaching multicolor optical immunolabels, *PNAS,* 97(3):996-1001 (2000)).

RESULTS

[60] Figure 11 (top) shows an adsorption spectrum typical of our colloid-coated APS slides. The absorption centered near 430 nm is typical of colloidal silver particles with sub-wavelength dimensions but not completely at the small particle limit. Figure 11 (bottom) shows a typical AFM image of the silver colloid coated APS coated glass slides. The colloid sizes are in the range 20-50 nm, which was expected from the preparation procedure (Turkevich et al, A study of the nucleation and growth processes in the synthesis of colloidal gold, *J. Discuss. Faraday Soc.*, 11:55-75 (1951), Henglein and Giersig, Formation of colloidal silver nanoparticles: capping action of citrate, *J. Phys. Chem. B,* 103:9533-9539; and Rivas et al, Growth of silver colloidal particles obtained by citrate reduction to increase the Raman enhancement factor, *Langmuir*, 17:574-577 (2001)). To determine whether these surface-bound colloids would enhance fluorescence, the surfaces were incubated with ICG-HSA to obtain a monolayer surface coating. The emission spectra showed a remarkable 30-fold larger intensity on the surfaces coated with silver colloids (Figure 12). The fluorescence intensities increased with the concentration of APS used to treat the cleaned surfaces (Figure 13), which also appeared to correlate with the optical density at 430 nm (not shown).

[61] In general, the enhancement of ICG emission seems to depend linearly, or at a higher power, on the amount of bound colloids. Theory has predicted that spaces between adjacent colloids may be more effective in increasing fluorescence intensity than isolated colloids (Gersten, J. I. and Nitzan, A, Photophysics and photochemistry near surfaces and small particles, *Surface Science,* 158:165-189 (1985)). Hence, it is expected that the ICG intensity to increase *more than linearly* with increasing colloid concentration. However, it is not clear if interacting colloids are superior in enhancing fluorescence.

[62] It is well known that some fluorophores, particularly those with some conformational freedom, display increased quantum yields in rigid environments. This mechanism seemed unlikely to explain the increased ICG intensity near silver colloids since ICG is bound to the protein, which is then bound to the glass or colloidal surface. Typically, a rigid environment results in decreased rates of non-radiative decay and thus longer lifetimes. In contrast, metallic surface-enhanced fluorescence is expected to result from increases in the rate of radiative decay, which will result in shorter lifetimes.

[63] Time-dependent intensity decays of ICG-HSA were measured in a cuvette (C) and when bound to glass (G) or silver colloids (S). The intensity decay is more rapid on glass than in bulk solution in a cuvette, and more rapid when immobilized on silver colloids as compared to on glass (Figure 14, top). At the present time, the lifetime reductions on glass is not completely understood, but this effect has been seen for several fluorophores (Lakowicz et al, Radiative decay engineering 2. Effects of silver island films on fluorescence intensity, lifetimes, and resonance energy transfer, *Anal. Biochem.*, 301:261-277 (2002) and Lakowicz et al, Intrinsic fluorescence from DNA can be enhanced by metallic particles, *Biochem. Biophys. Res. Commun.*, 286:875-879 (2001)). The reduced lifetimes on colloids is due to a

rapid 59 ps dominant component in the decay, which can be seen from the fitted parameters (See Table 2 below).

Table 2

Analysis of the intensity decay of ICG-HSA in buffer, on glass and on laser deposited silver, measured using the reverse start-stop time-correlated single photon counting technique. The data was analysed in terms of the multi-exponential model, c.f. Eq. 1.

Sample	α_i	τ_i (ns)	f_i	$\bar{\tau}$ (ns)	$\langle\tau\rangle$ (ns)	χ_R^2
In Buffer	0.158	0.190	0.05	-	-	
	0.842	0.615	0.95	0.592	0.548	1.4
On Glass	0.655	0.078	0.205	-	-	
	0.345	0.578	0.795	0.476	0.251	0.92
Laser deposited Ag	0.999	0.006	0.157	-	-	
	0.004	0.146	0.165	-	-	
	0.006	0.399	0.678	0.296	0.035	1.08

[64] The impulse response functions, which are the decays which would be observed with an infinity short instrument response function (RF), are shown in Figure 14. The contribution of the 59 ps component accounts for 14.7 % of the total steady-state ICG intensity and decreases with the amplitude-weighted lifetime from 325 ps to 68 ps on glass and silver colloids respectively (see Table 2).

[65] Applicants questioned whether the short component in the ICG intensity decay was due to scattered light. Metallic colloids are known to be strongly scattering (Yguerabide and Yguerabide, Light-scattering submicroscopic particles as highly fluorescent analogs and their use as tracer labels in clinical and biological applications, I. Theory, *Anal. Biochem.*, 262:137-156 (1998), Yguerabide and Yguerabide, Light-scattering submicroscopic particles as highly fluorescent analogs and their use as tracer labels in clinical and biological

applications, II. Experimental characterization, *Anal. Biochem.*, 262:157-176 (1998), Schultz et al, Single-target molecule detection with nonbleaching multicolor optical immunolabels, PNAS, 97(3):996-1001 (2000)). Control measurements of the glass or colloid-coated slides, without ICG-HSA, yielded a background of much less than 1% when observed through the combination of filters used to isolate the ICG emission. Applicants further examined the possibility of scattered light by recording the emission spectra *through* the emission filter used for the time-resolved measurements (Figure 15). These spectra showed no intensity at the excitation wavelength of 760 nm, demonstrating that scattered light is not the origin of the short lifetime components of ICG on colloid-coated slides. However, this was expected as the pulse width of the 760 nm Pyridine 2 dye laser was <5 ps. Applicants thus assigned the short component to those ICG molecules which have the appropriate proximity and orientation relative to the silver surface to display increased rates of radiative decay. Since only a fraction of the total emission displays the 59 ps component, and since much of the decay occurs with a lifetime similar to that on glass, it is probable that the 30-fold increase in intensity seen in Figure 12 is due to a sub-population of the ICG molecules which display greater than 30-fold enhancements.

[66] Another favorable aspect of metal-enhanced fluorescence is the possibility of increased photostability (Lakowicz, Radiative decay engineering: Biophysical and biomedical applications, *Anal. Biochem.*, 298:1-24 (2001)). Photochemical reactions occur while the fluorophores are in the excited state, so it is expected that decreased lifetimes should result in an increased photostability. To be more precise, the actual photodecomposition rate may be unchanged, but if the fluorophore returns to the ground state more quickly, there is less time and therefore a lower possibility, of reactions per excitation de-excitation (emission) cycle.

[67] The photostability of ICG-HAS was examined by recording the steady state intensity with continuous vertically polarized 760 nm illumination. When illuminated with the same incident intensity (Figure 16, top) the intensity of ICG-HSA on glass or colloids were equally photostable. This suggests that the increased intensity seen on the colloids is not due to an increased rate of excitation, which would be expected to result in more rapid photobleaching. The photostability with the incident light intensities adjusted to result in the same emission intensity (Figure 16, bottom), which in this case is a 30-fold lower incident intensity for the colloid-coated surfaces, was also examined. These results suggest that each ICG molecule can result in at least 30-fold more detectable signal prior to photobleaching, which could be useful for low copy number assays. Note for Figure 16 bottom that the excitation intensity has been attenuated ≈30-fold, but for comparison, this data has been re-normalized to give a similar intensity as in Figure 16 (top).

DISCUSSION

[68] As described in the Background of the Invention, increased intensity from ICG can result in improved imaging to the retinal vasculature. Additional applications include higher intensity ICG probes and as a contrast agent for optical medical tomography. Since the seminal report by Chance and co-workers (Ntziachristos et al, Concurrent MRI and diffuse optical tomography of breast after indocyanine green enhancement, *PNAS*, 97(6):2767-2772 (2000)) there has been intense interest in the use of diffusely scattered red-NIR light for imaging and *in vivo* physiological monitoring (Sevick-Muraca et al, Fluorescence and absorption contrast mechanisms for biomedical optical imaging using frequency-domain techniques, *Photochem. Photobiol.*, 66(1):55-64 (1997) and Becker et al, Macromolecular contrast agents for optical imaging of tumors: Comparison of indotricarbocyanine-labeled human serum albumin and transferrin, *Photochem. Photobiol.*, 72(2):234-241 (2000)). These

effects include both steady state and time-resolved measurements of the scattered light. While much progress has been made, it is becoming apparent that the contrast in tissues from the red-NIR light is often too small for imaging. As a result there is growing interest in the use of optical contrast agents which remain in the blood vessels or display localized emission due to selective binding or enzymatic activity. The >30-fold increase in ICG intensity found near silver colloids is useful for optical contrast in tissues.

[69] The *in-vivo* use of colloids suspensions depends upon low or minimal toxicity. Applicants were unable to find publications which describe the toxicity of injected silver colloids directly. However, less direct evidence suggests low toxicity. Colloid silver has been used as an ingestable medicine for over 100 years due to its antimicrobial activity and is still used today to treat or present eye infections in infants. Sublingual silver colloids are thought to appear rapidly in the bloodstream with no reported toxic effects. Lozenges containing silver nitrate and used as an aid to cease smoking (Bromberg et al, Sustained release of silver from periodontal wafers for treatment of periodontitis, *J. Controlled Rélease*, 68(1):63-72 (2000) and Lancaster and Stead, Silver acetate for smoking cessation, *Cochrane Database System Rev.*, 2:CD000191 (2000)). It seems probable that some of the silver ions used in this regard become reduced to metallic silver. In addition silver is in widespread use for sealing dental cavities. The only report of toxicity is for an individual, already ill, who injected silver nitrate anti-smoking tablets for 40 years (Ohbo et al, Argyria and convulsive seizures caused by ingestion of silver in a patient with schizophrenia, *Psychiatry & Clinical Neurosciences*, 50(2):89-90 (1996)). Based on this experience and lack of evidence, it seems probable that colloidal silver would be medically safe as an injectable.

[70] The particles (colloids) may be injected themselves. Protein-size particles are currently being used in a variety of medical applications. Liposome and polymers particles

are used for drug delivery (Wang and Wu, Preparation and characterization of agarose hydrogel nanoparticles for protein and peptide drug delivery, *Pharmaceutical Dev. & Technol.*, 2(2):135-142 (1997) and Hood et al, Tumor regression by targeted gene delivery to the neovasculature, *Science*, 296:2404-2407 (2002)) and magnetic particles are being tested for contrast agents for MRI (Adzamli et al, Preliminary evaluation of a polyethyleneglycol-stabilized manganese-substituted hydroxylapatite as an intravascular contrast agent for MR angiography, *J. Magnetic Resonance Imaging*, 7(1):204-208 (1997) and Josephson et al, A functionalized superparamagnetic iron oxide colloid as a receptor directed MR contrast agent, *J. Magnetic Resonance Imaging*, 8(5), 637-646 (1990)).

LIGHT DEPOSITED METALLIC PARTICLES

[71] The present invention also relates to metallic surfaces or particles deposited by laser illumination. The use of metallic surfaces or particles deposited by laser illumination is not limited to the use of indocyanine green discussed above. Examples of uses for metallic surfaces or particles deposited by laser illumination include fluorescent probes or assays as discussed in the Background of the Invention Section above.

MATERIALS AND METHODS

[72] ICG is chemically and photochemically unstable and thus provides an ideal opportunity to test photo-deposited silver for both metal-enhanced emission and increased photochemical stability.

[73] ICG and HSA were obtained from Sigma and used without further purification. Emission spectra of ICG were measured using a SLM 8000 spectrofluorometer with an excitation wavelength of 760 nm from a Spectra Physics Tsunami Ti:Sapphire laser in the CW (non-pulsed) mode, vertically polarized, 760 nm incident on the sample at 45° from the normal. Emission spectra were recorded at the magic angle. Intensity decays were also

measured at the magic angle, 54.7°, by time-correlated single photon counting (TCSPC), using a SPC630 PC card (Becker and Hickl Gmbh), in reverse start-stop mode. 760 nm excitation was obtained from a mode-locked Argon-ion pump, cavity dumped Pyridine 2 dye laser with 3.77 MHz repetition rate. The instrumental response function was < 40 ps fwhm.

[74] For the laser deposition of silver particles, clean glass substrates were silanized with 3-aminopropyl trimethoxysilane (APS) or 3-mercaptopropyl trimethoxysilane (MCTMS). Glass microscope slides (Aldrich Chemical Co.) were first cleansed in a 10:1 (v/v) mixture of H_2SO_4 (98%) and H_2O_2 (30%). The slides were subsequently treated with an appropriate % volume / volume (v/v) silanization agent for one hour to form the adhesion layer on the glass substrate. Water or ethanol were used to form the silanization solution for APS and MCTMS respectively. This treatment coats the glass surface with either amine groups, in the case of APS, or thiol groups, for MCTMS, which are well- known to bind to silver colloids from solution. After washing in distilled water to remove excess agents, the slides were then ready for the laser deposition of silver.

[75] The silver colloid forming solution was prepared by adding 4 ml of 1 % trisodium citrate solution to a warmed 200 ml of 10-3 M $AgNO_3$ solution. This warmed solution already contains some silver colloids as seen from a surface plasmon absorption optical density near 0.1. A 180 μL aliquot of this solution was syringed between the glass microscope slide and plastic cover slip (CoverWell PCI 0.5) which created a micro-sample chamber 0.5 mm thick (Figure 17). For all experiments a constant volume of 180 μL was used. Irradiation of the sample chamber was undertaken using a HeCd laser, Liconix Model 4240PS, with a power ~ 8 mW, which was collimated and defocused using a microscope objective 10x NA 0.40 to provide a illumination over a 0.5 mm diameter spot. The diameter of the illuminated region waas ~5 mm. Following silver deposition, the slides were rinsed

and incubated for 24 hours in a 30 μM ICG, 60 μM HSA buffered solution. The HSA-ICG coated slides were then sandwiched with another uncoated glass microscope slide which formed a microcuvette, with an approximate 1 micron path length. Buffer in the small cavity prevented the HSA-ICG above silver and on the glass (unsilvered areas) from drying out during measurements.

RESULTS

[76] Illumination of the APS and MCTMS treated slides at 442 nm resulted in the deposition of metallic silver in the illuminated region. Laser-deposited silver could be seen visually within minutes, however deposited silver could not be observed with room light exposure for a similar period of time. However over much longer time periods, e.g. 4 days, silver was evident on the glass slides, suggesting that even ambient room light can produce silver colloids, which can adhere to the surfaces over much longer time periods. To some extent this observation also manifests itself in the fact that bottles of long-standing silver nitrate on a laboratory shelf are coated with metallic silver over time.

[77] The laser-deposited silver displayed a surface plasmon absorption (Figure 18) typical of sub-wavelength size silver particles. Silver was deposited on both the microscope slide and the cover slip, but significantly more silver was visible on the treated slides than on the untreated cover slip. The optical density of the deposited silver increased approximately linearly with illumination time (data not shown), increasing much more rapidly with MCTMS treated slides (data not shown).

[78] The emission spectrum of ICG-HSA when bound to illuminated or non-illuminated regions of the APS and MCTMS treated slides was examined. For APS treated slides (Figure 19), the intensity of ICG was increased about 7-fold in the regions with laser-deposited silver. The extent of the ICG enhancement was variable from spot-to-spot, or within a single spot,

with some regions displaying much higher increases in intensity which appeared to depend on the optical density of the spot. It was generally observed, within a single spot, that the ICG intensity increased towards the center of the spot, although no qualitative data is available due to the diameter of the excitation beam with respect to that of the spot itself. It appears that the enhancement is likely to follow the Gaussian nature of the beam profile.

[79] Fluorescent probes frequently display increases in intensity when bound in a rigid environment. In such cases the increased intensity is due to a decrease in the non-radiative decay rates, knr, so that the lifetime also increases. See Formula (6).

[80] In contrast, the increased intensities due to a metallic surface, Q_m are due to an increase in the radiative decay rate ($\Gamma+\Gamma_m$), and thus result in increased quantum yields and decreased lifetimes, τ_m. See Formulae (7) and (8).

[81] For completeness, it is noted that other effects of metals are possible including quenching and increased rates of excitation.

[82] To distinguish between increases in k_{nr} or increase in Γ_m, the intensity decays of ICG-HSA was examined (Figure 20). The intensity decay is more rapid on glass than in solution. This effect has been observed previously, but Applicants presently have not have an explanation. More importantly, there is a much more dramatic decrease in the decay times when ICG-HSA is bound to laser-deposited silver (Figure 20 and Table 3).

Table 3

[83] Analysis of the intensity decay of ICG-HSA in buffer, on glass and on laser deposited silver, measured using the reverse start-stop time-correlated single photon counting technique. The data was analyzed in terms. of the multi-exponential model, c.f. eq. 1.

Sample[a]	α_i	τ_i (ns)	f_i	$\bar{\tau}$ (ns)	$<\tau>$(ns)	χ^2_R

In Buffer	0.158	0.190	0.05	-	-	
	0.842	0.615	0.95	0.592	0.548	1.4
On Glass	0.655	0.078	0.205	-	-	
	0.345	0.578	0.795	0.476	0.251	0.92
Laser deposited Ag	0.999	0.006	0.157	-	-	
	0.004	0.146	0.165	-	-	
	0.006	0.399	0.678	0.296	0.035	1.08

[84] The decrease in the decay times τ and <τ> are due to a very short, ~ 6 ps component in the decay, with the other minor components similar to that observed on glass. Control measurements showed that scattered light did not contribute to the intensity decays and therefore were not the origin of the shorter components of the decay. The short component is interpreted as due to ICG molecules at approximate distances from the silver surfaces to result in a dramatic increased radiative decay rate, and the longer component to ICG molecules more distant from the silver surfaces. The fact that the lifetimes decreased indicates that at least part of the intensity increase is due to faster radiative decay and not an increased rate of excitation.

[85] The photostability of ICG-HSA when bound to glass or laser-deposited silver was also examined. It was reasoned that ICG molecules with shortened lifetimes should be more photostable because there is less time for photochemical processes to occur. The intensity of ICG-HSA was recorded with continuous illumination at 760 nm. When excited with the same incident power the fluorescence intensities, when considered on the same intensity scale, decreased somewhat more rapidly on the silver (Figure 21, top). However, the difference is minor. Since the observable intensity of the ICG molecules prior to photobleaching is given by the area under these curves it is evident at least 10-fold more

signal can be observed from ICG near silver as compared to glass. Alternatively, one can consider the photostability of ICG when the incident intensity is adjusted to result in the same signal intensities on silver and glass. In this case (Figure 21, bottom) photobleaching is slower on the silver surfaces. The fact that the photobleaching is not accelerated for ICG or silver indicates that the increased intensities on silver are not due to an increased rate of excitation.

[86] Using an inverted microscope to laser deposit silver on APS-treated slides was investigated, with the intention of producing significantly smaller spots than the 0.5 cm diameter spots obtained with the 8 mW illumination using the HeCd source (Figure 17). By adapting an inverted microscope, Axiovert 135 TV, (Figure 22 - top) and using a 10x 0.4 NA objective, the rapid production of laser deposited spots of the order of 50 μm diameter, (Figure 22 - bottom), with different optical densities depending on the time of illumination, was obtained. If the slides were not treated with APS, silver was deposited. However, the silver was less strongly bound to the glass surface and could be removed with washing. Interestingly, due to the increased irradiance of the focused light, ~ 560 W/cm2, the silver now deposited much faster on the slides (Figure 22 - bottom). Thus obtaining the application of highly focused light for the laser deposition of silver over very small areas and indeed, in a very short time frame. The speed of this silver lithographic process aids MEF technologies and their mass production, such as for disposable sensors, gene chips or microfluidic type devices.

DISCUSSION

[87] Metal-enhanced fluorescence from light-deposited silver can have numerous applications in analytical chemistry, medical diagnostics and biotechnology, including microfluidic devices such as the "lab on a chip". See, for example, Liu et al, DNA

amplification and hybridization assays in integrated plastic monolithic devices, *Anal. Chem.*, 74:3063-3070 (2002), Yakovleva et al, Microfluidic enzyme immunoassay using silicon microchip with immobilized antibodies and chemiluminescence detection, *Anal. Chem.*, 74:2994-3004 (2002), Verpoorte, Microfluidic chips for clinical and forensic analysis, Electrophoresis, 23:677-712 (2002), Anderson et al, A miniature integrated device for automated multistep genetic assays, *Nucleic Acids Res.*, 28(12):e60-eoa (2002) and Wallraff et al, DNA sequencing on a chip, *Chemtech.*, 27:22-32 (2002). In these devices there are typically spatially separate mixing and detector locations. The detection areas may be illuminated to deposit silver for increased sensitivity detection, particularly for low quantum yield fluorophores which are preferentially enhanced near silver particles. (Lakowicz, Radiative decay engineering: Biophysical and biomedical applications, *Anal. Biochem.*, 298:1-24 (2001), Lakowicz et al, Radiative decay engineering 2. Effects of silver island films on fluorescence intensity, lifetimes, and resonance energy transfer, *Anal. Biochem.*, 301:261-277 (2002), Lakowicz et al, Intrinsic fluorescence from DNA can be enhanced by metallic particles, *Biochem. Biophys. Res. Commun.*, 286:875-879 (2002), Gryczynski et al, Multiphoton excitation of fluorescence near metallic particles: Enhanced and localized excitation, *J. Phys. Chem. B*, 106:2191-2195 (2002) and Schalkhammer et al, Detection of fluorophore-labeled antibodies by surface-enhanced fluorescence on metal nanoislands, SPIE, 2976:129-136 (1997)).

[88] This approach may also be applied to other fluorescence systems such as flow DNA analysis or single molecule DNA sequencing (Van Orden et al, Single-molecule identification in flowing sample streams by fluorescence burst size and intraburst fluorescence decay rate, *Anal. Chem.*, 70:1444-1451 (1998), Van Orden et al, High-throughput flow cytometric DNA fragment sizing, *Anal. Chem.*, 72:37-41 (2000), Saueret al, Single molecule DNA sequencing

in submicrometer channels: state of the art and future prospects, *J. Biotechnol.*, 86:181-201 (2001), and Stephan et al, Towards a general procedure for sequencing single DNA molecules, *J. Biotechnol.*, 86:255-267 (2001)).

[89] Another application of light-deposited silver may be on gene chips or DNA arrays (Schena et al, Microarrays: biotechnology's discovery platform for functional genomics, *Tibtech*, 16:301-306 (1998) and Brown and Botstein, Exploring the new world of the genome with DNA microarrays, Nature Genet. Supp., 21:33-37 (1999)). In this application photolithography is already in use for spatially directed synthesis of the DNA oligomers (Lipschutz et al, High density synthetic oligonucleotide arrays, Nature Genet. Supp., 21:20-214 (1999)).

[90] It is possible to use the illumination steps to deposit silver at desired locations. Alternatively, the substrate may be marked, such as by microcontact printing of silane reagents onto glass providing the desired spatial distribution of metallic particle locations. For example, Biju et al discloses microcontact printing with amino groups. Biju et al, Fluorophore modified microcontact prints: A methodology for readout using fluorescence microscopy, J. Imaging Science and Technology, 46(2):155-158 (2002)). The entire device may be illuminated to obtain deposition of the colloids on the reagent-coated regions.

[91] All of the references and journal articles are hereby incorporated by reference herein in their entirety.

WHAT IS CLAIMED IS:

1. A material comprising

a cyanine dye-albumin conjugate and

a metallic particle,

wherein said cyanine dye-albumin conjugate is attached to said metallic particle such that the metallic particle provides an enhancement of the fluorescence of the indocyanine dye upon exposing said material to irradiation.

2. The material of claim 1, wherein said cyanine dye-albumin conjugate is an indocyanine green-albumin conjugate.

3. The material of claim 2, wherein said metallic particle is coated on a surface of a first substrate.

4. The material of claim 3, wherein said metallic particle is coated on said first substrate from a metallic colloid.

5. The material of claim 3, wherein said metallic particle is attached to said first substrate through a compound containing an amino group.

6. The material of claim 3, wherein said compound containing an amino group is 3-aminopropyltrimethoxysilane.

7. The material of claim 3, wherein said substrate comprises quartz or glass.

8. The material of claim 1, wherein said metallic particle comprises silver.

9. The material of claim 1, wherein said metallic particle comprises gold.

10. The material of claim 3, further comprising

a second substrate,

a metallic particle coated on a surface of said second substrate and

an indocyanine dye-albumin conjugate attached to said metallic particle, wherein said first and second substrates are positioned apart from each other such that said coated surfaces face each other.

11. The material of claim 10, wherein the distance between said surfaces of said first and second substrates is about 1 micrometer apart.

12. The material of claim 1, wherein said albumin is human serum albumin.

13. The material claim 1, wherein said material is sensitive to a selected pH, a selected anion, a selected cation or is magnetized.

14. The material of claim 1, wherein said metallic colloid selectively binds or exhibits enzymatic attraction.

15. The material of claim 1, wherein said metallic particle is spherical.

16. A system comprising

an cyanine dye-albumin conjugate and

a metallic particle,

wherein said indocyanine dye-albumin conjugate and said metallic particle are positioned at a distance sufficient to provide an enhancement of the fluorescence of the indocyanine dye upon exposing said system to irradiation.

17. The system of claim 16, wherein said cyanine dye-albumin conjugate is an indocyanine green-albumin conjugate.

18. The system of claim 16, the distance between said cyanine dye and said metallic particle is 40 to 90 Å.

19. A material comprising

a substrate,

at least one metallic particle attached to a surface of said substrate,

albumin coated on said at least one metallic particle and said surface of said substrate, and

a cyanine dye bound to said albumin,

wherein said metallic particle provides an enhancement of the fluorescence of the indocyanine dye upon exposing said material to irradiation.

20. The material of claim 19, wherein said cyanine dye is indocyanine green.

21. A metallic colloid comprising a cyanine dye-albumin conjugate and at least one metallic particle, wherein said at least one metallic particle provides an enhanced fluorescence intensity of the indocyanine dye upon exposing said metallic colloid to irradiation.

22. The metallic colloid of claim 21, wherein said cyanine dye-albumin conjugate is an indocyanine green-albumin conjugate.

23. The metallic colloid of claim 21, wherein said cyanine dye-albumin conjugate is attached to said metallic particle.

24. The metallic colloid of claim 21, wherein said albumin is human serum albumin.

25. The metallic colloid of claim 21, further comprising blood.

26. The metallic colloid of claim 21, wherein said metallic colloid is sensitive to a selected pH, a selected anion, a selected cation or is magnetized.

27. The metallic colloid of claim 21, wherein said metallic colloid selectively binds or exhibits enzymatic attraction.

28. The metallic colloid of claim 21, wherein said metallic colloid selectively binds or exhibits enzymatic attraction.

29. A method of imaging or assaying comprising administering the colloid of claim 21 to a subject and irradiating said subject to detect the presence of indocyanine dye.

30. The method of claim 29, wherein said cyanine dye is bound to said albumin prior to injecting the colloid.

31. The method of claim 29, wherein said indocyanine dye is administered intravenously.

32. The method of claim 29, wherein said imaging or assaying is retinal angiography, measurement of plasma volume, blood volume, measurement of cardiac output, measurement of photocoagulation, assessment of burn depth/severity, measurement of liver function, measurement of exercise physiology, guiding of biopsy, optical tomography, optical tumor detection, or choridal imaging.

33. A method of imaging or assaying comprising administering a colloid comprising a metallic particle and a cyanine dye to a subject, forming a bond between said indocyanine dye and albumin present in said subject *in vivo* and irradiating said subject to detect the presence of cyanine dye.

34. The method of claim 33, wherein said cyanine dye is indocyanine green.

35. The method of claim 33, wherein said albumin is human serum albumin.

36. A method of detecting a presence of or quantifying an amount of cyanine dye comprising contacting a solution comprising a cyanine dye-albumin conjugate with a substrate containing a metallic particle thereon and irradiating the substrate to detect the presence of or to measure the amount of cyanine dye in said solution.

37. The method of claim 36, wherein said cyanine dye-albumin conjugate is an indocyanine green-albumin conjugate.

38. The method of detecting a presence of or quantifying an amount of cyanine dye of claim 36, further comprising washing prior to irradiating the substrate.

39. A method of detecting a presence of or quantifying an amount of indocyanine comprising contacting a solution comprising an indocyanine dye with a substrate containing at least one metallic particle with a film of albumin thereon and irradiating the substrate to detect the presence of or to measure the amount of indocyanine dye in said solution.

40. The method of detecting a presence of or quantifying an amount of indocyanine indocyanine of claim 32, further comprising washing prior to irradiating the substrate.

41. A method of making an apparatus for detecting or measuring the presence of a compound capable of fluorescing in a sample, comprising

contacting a substrate with a solution comprising silver and

irradiating said substrate with laser irradiation to deposit a metallic surface or to deposit one or more metallic particles on said substrate.

42. The method of claim 41, wherein said solution comprises $AgNO_3$.

43. The method of claim 42, wherein said solution comprises a mild potential reducing agent selected from the group consisting of a surfactant and dimethylformamide.

44. The method of claim 42, further comprising adding a film spacer layer over said substrate with the metallic surface or the one or more metallic particles deposited thereon.

45. The method of claim 44, wherein said film spacer layer is selected from the group consisting of silica, a PVA polymer film and albumin.

46. The method of claim 42, further comprising incubating said substrate with the metallic surface or the one or more metallic particles deposited thereon with a buffered solution comprising albumin.

47. The method of claim 41, wherein said substrate is irradiated by said laser irradiation at one or more discrete selected locations and said metallic surface or said one or more metallic particles are deposited at the location of said laser irradiation.

48. The method of claim 47, wherein the diameter of said metallic surface or said one or more metallic particles is 0.5 mm or less.

49. The method of claim 47, wherein the diameter of said metallic surface or said one or more metallic particles is 50 μm or less.

50. The method of claim 41, wherein said substrate is coated with a silanization agent.

51. The method of claim 50, wherein said silanization agent comprises an amino group or a thiol group.

52. The method of claim 50, wherein said silanization agent is selected from the group consisting of 3-aminopropyl trimethoxysilane and 3-mercaptopropyl trimethoxysilane.

53. The method of claim 41, further comprising selectively coating said substrate with a silanization agent at one or more discrete locations and wherein said substrate is irradiated with said laser irradiation to deposit said metallic surface or to deposit said one or more metallic particles on said substrate at said one or more discrete locations.

54. The method of claim 53, wherein said silanization agent is selectively coating said substrate by microcontact printing.

55. A system comprising an optochemical fluorescence measuring apparatus and an analyte-specific fluorescent compound for measuring the concentration of an analyte in a sample,

said optochemical fluorescence measuring apparatus comprising a substrate, an island layer consisting of islands of an electrically-conductive material deposited by laser irradiation

on the substrate, said islands having a diameter of less than 300 nm; a biorecognitive layer applied to said island layer; said biorecognitive layer being capable of binding with said analyte; and

said analyte-specific fluorescent compound having a quantum yield which increases in the vicinity of said island layer.

56. An apparatus for detecting or measuring the presence of a compound capable of fluorescing in a sample comprising a metal in the form of a particle or a film on a substrate, at least one film spacer layer, said compound capable of fluorescing, and a source of irradiation, wherein the metal particle or metal film and the compound are separated by said at least one film spacer layer and

wherein said metal in the form of a particle or a film on the substrate is deposited on the substrate by laser irradiation.

57. A method for detecting the presence of a compound comprising

contacting an apparatus of claim 56 with a composition comprising said compound wherein the compound is spaced at a distance from a metal particle with the film spacer layer;

exposing the compound to radiation; and

detecting the fluorescent emission,

wherein the distance provides an enhanced fluorescence intensity of the compound.

58. A system comprising a test sample and the apparatus of claim 1, wherein said test sample comprises one or more biomolecule, and wherein said one or more metal particles and at least one of said one or more biomolecule in said test sample are positioned at a distance apart sufficient to affect intrinsic emission of electromagnetic radiation of at least one of said one or more biomolecule upon exposing said system to exciting electromagnetic radiation.

59. The system of claim 58, wherein said biomolecule is attached to an extrinsic fluorophore.

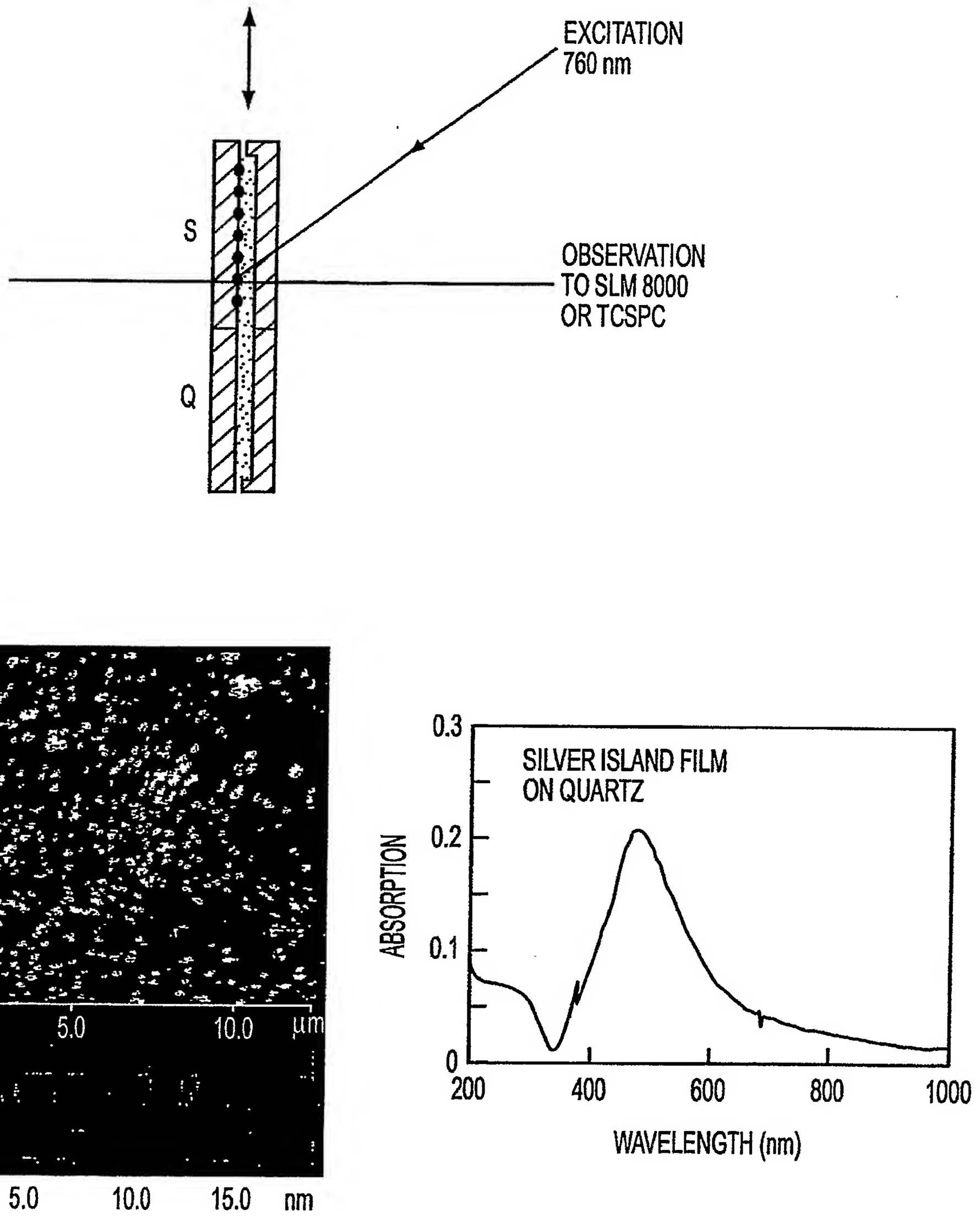
EXCITATION
760 nm
S
Q
OBSERVATION
TO SLM 8000
OR TCSPC
100
0
-100
0
5.0
10.0
15.0
µm
nm
SILVER ISLAND FILM
ON QUARTZ
ABSORPTION
0.3
0.2
0.1
0
200
400
600
800
1000
WAVELENGTH (nm)

FIG. 1

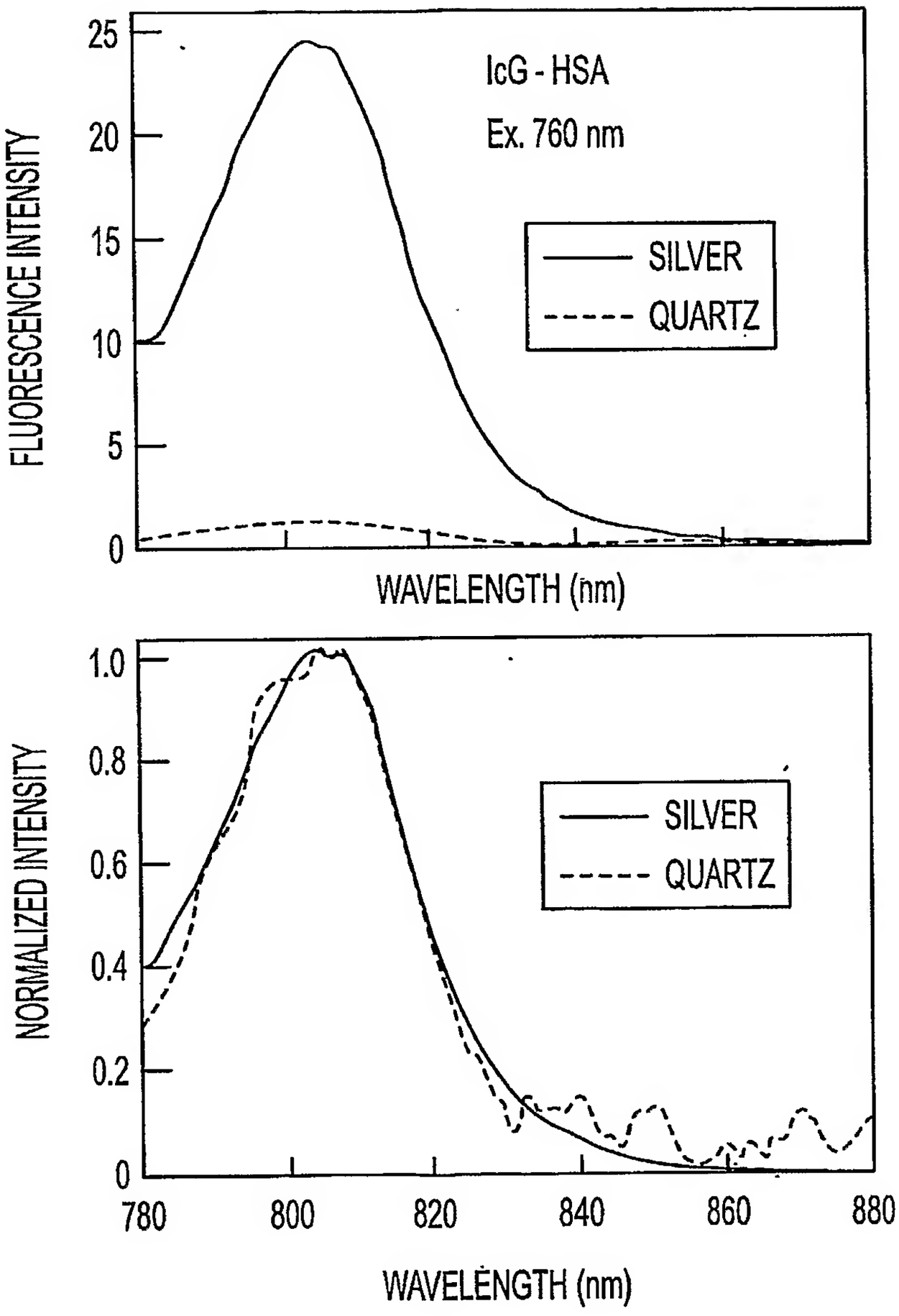
IcG - HSA
Ex. 760 nm
SILVER
QUARTZ
FLUORESCENCE INTENSITY
25
20
15
10
5
0
WAVELENGTH (nm)
NORMALIZED INTENSITY
1.0
0.8
0.6
0.4
0.2
0
780
800
820
840
860
880
SILVER
QUARTZ
WAVELENGTH (nm)

FIG. 2

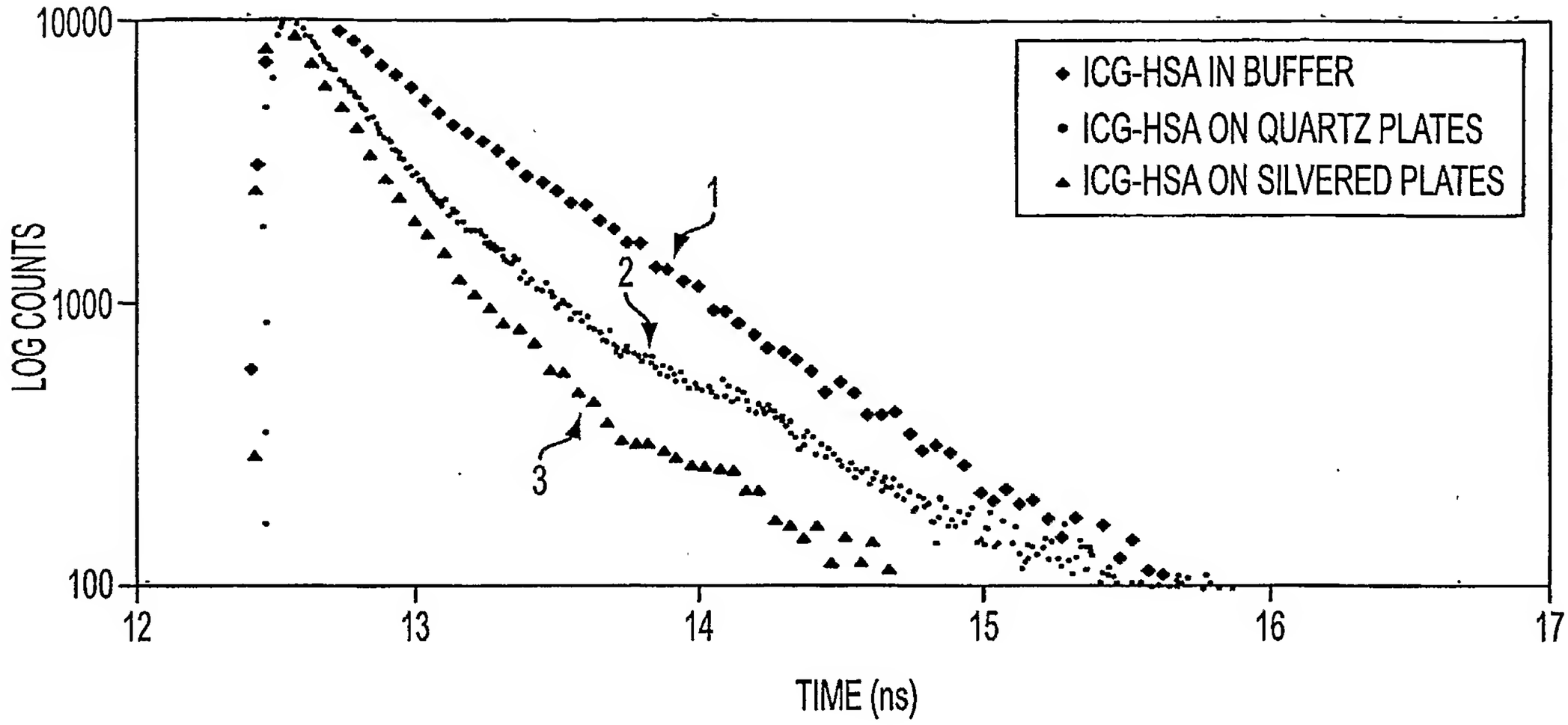
10000
1000
100
LOG COUNTS
12
13
14
15
16
17
TIME (ns)
ICG-HSA IN BUFFER
ICG-HSA ON QUARTZ PLATES
ICG-HSA ON SILVERED PLATES
1
2
3

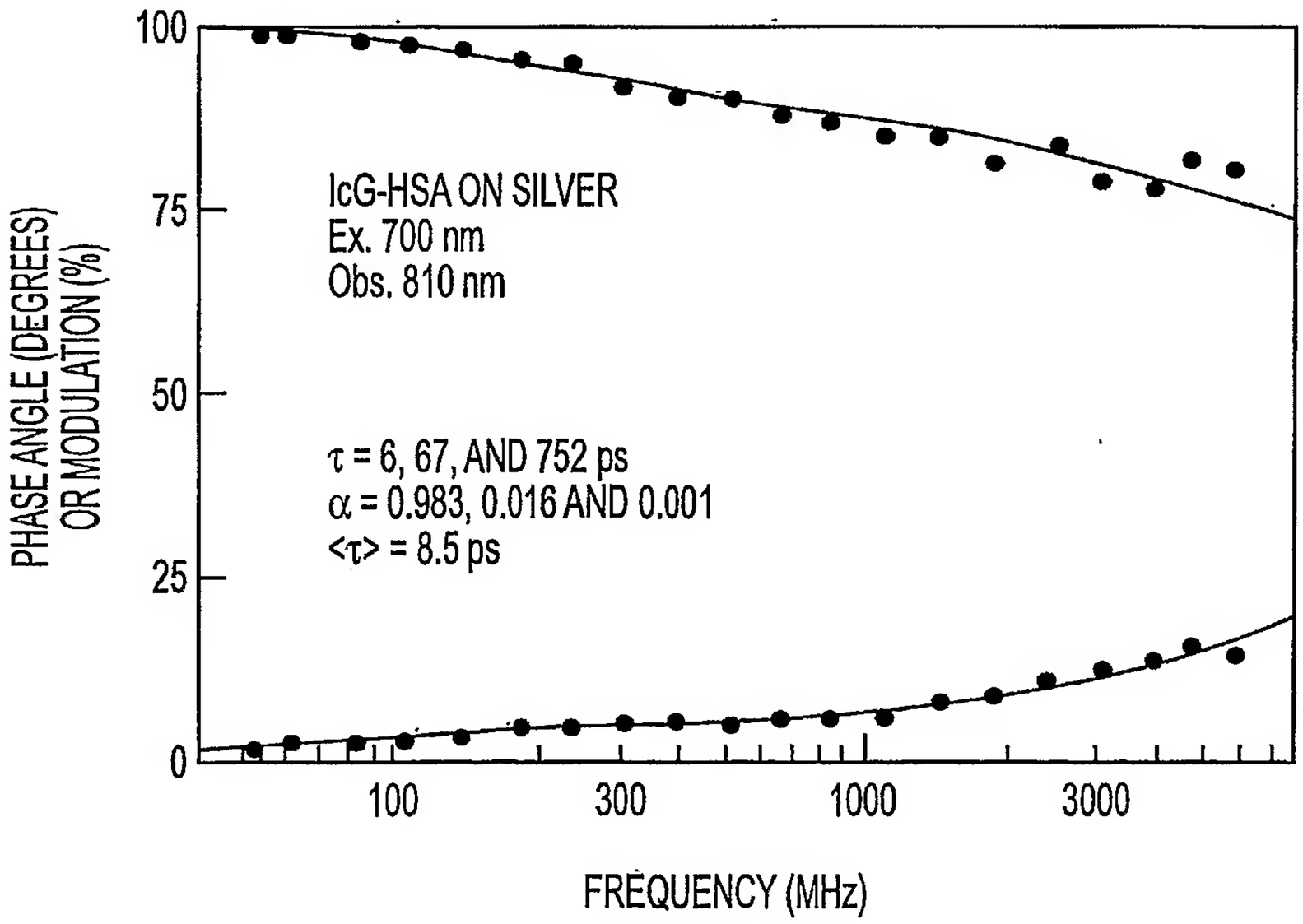
100
75
50
25
0
PHASE ANGLE (DEGREES)
OR MODULATION (%)
IcG-HSA ON SILVER
Ex. 700 nm
Obs. 810 nm
τ = 6, 67, AND 752 ps
α = 0.983, 0.016 AND 0.001
<τ> = 8.5 ps
100
300
1000
3000
FREQUENCY (MHz)

FIG. 3

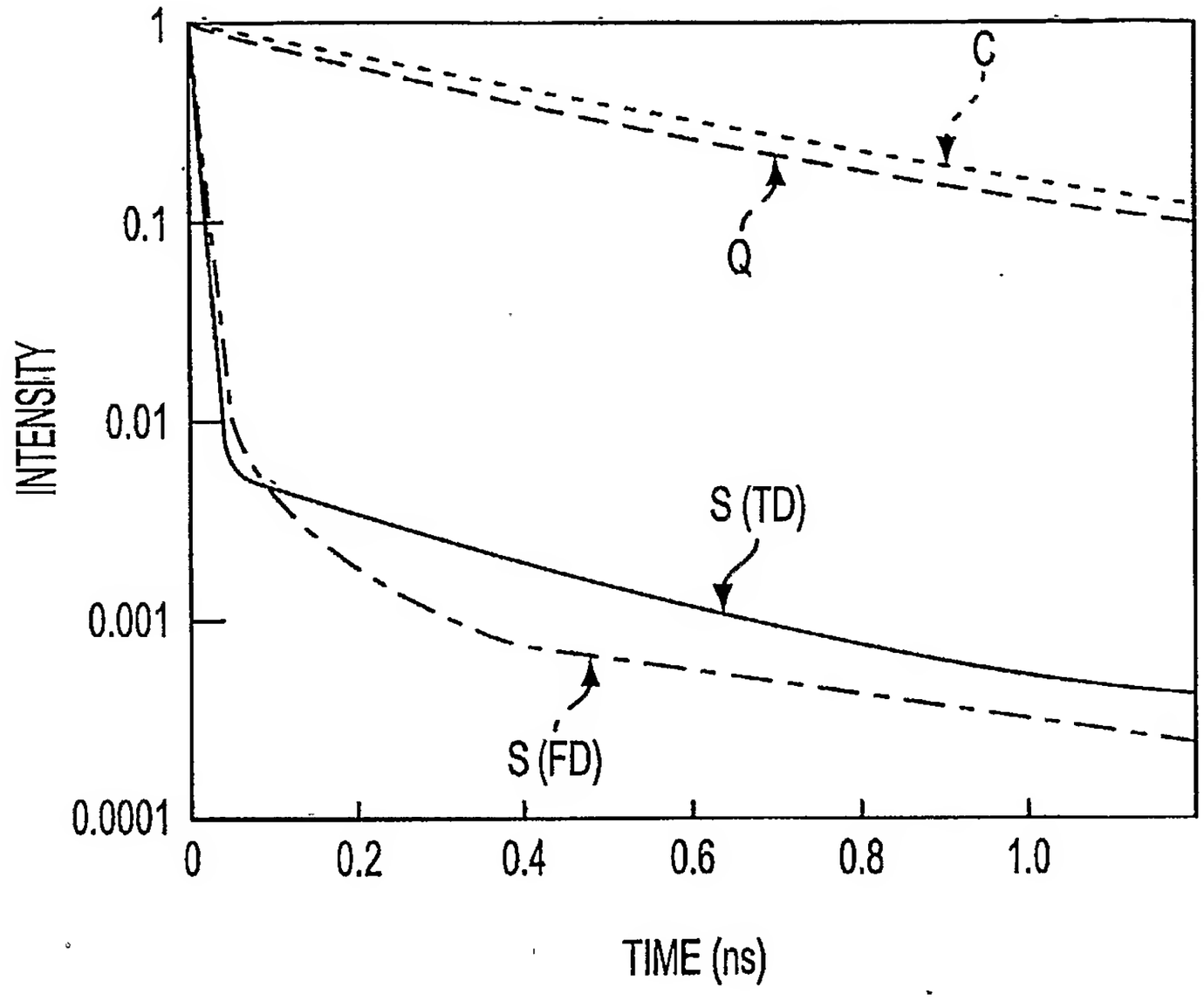

FIG. 4

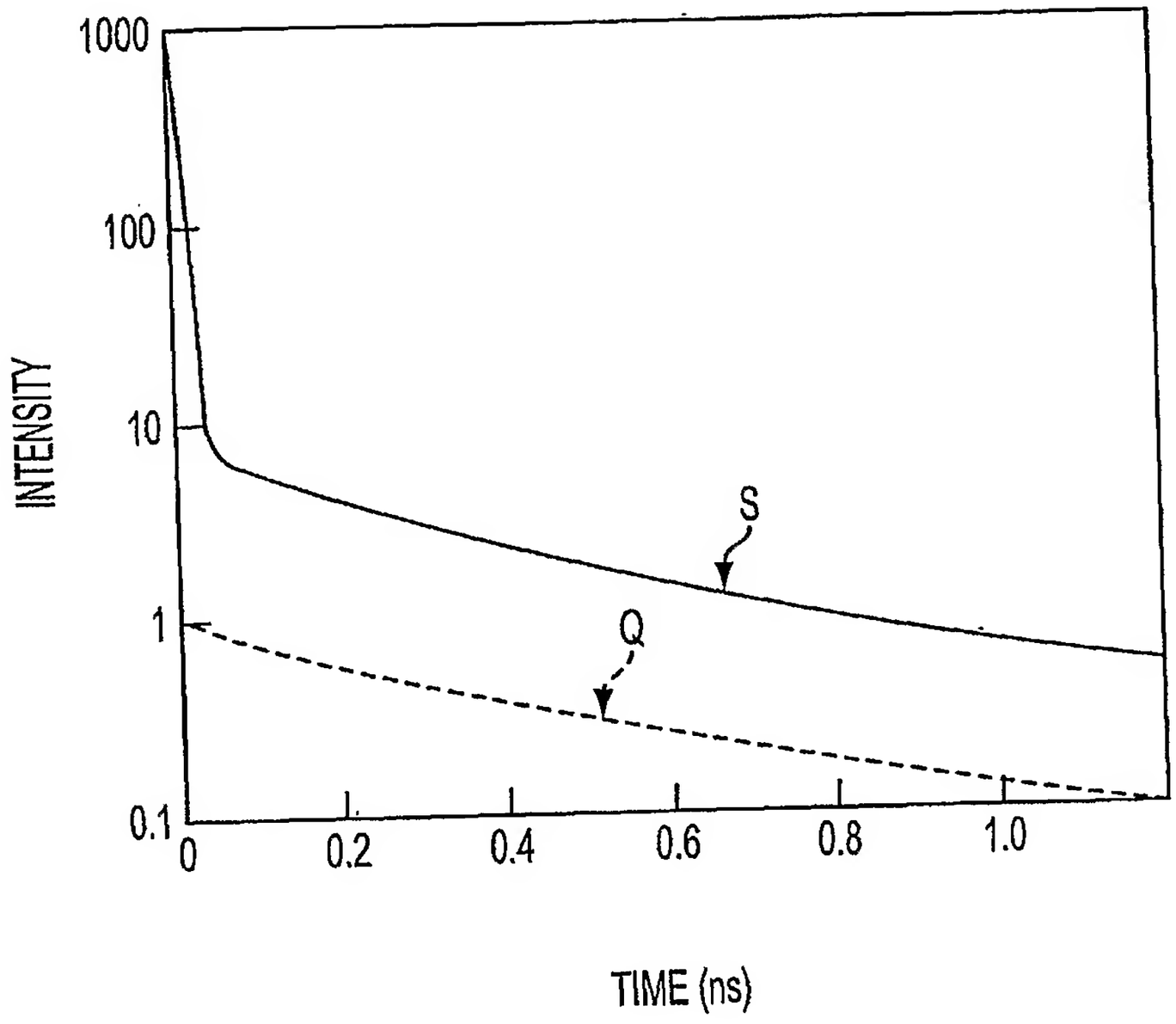

FIG. 5

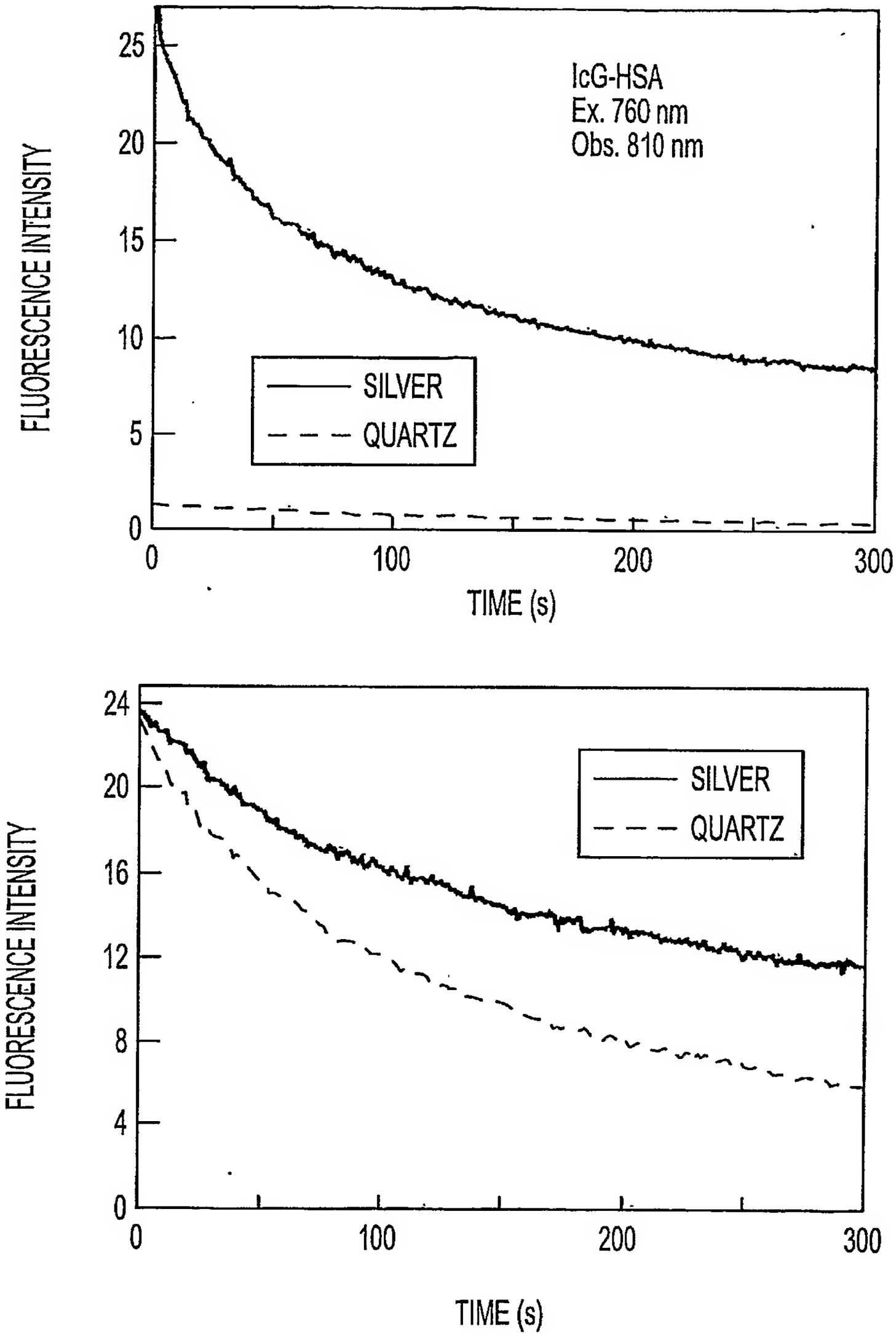
IcG-HSA
Ex. 760 nm
Obs. 810 nm
SILVER
QUARTZ
FLUORESCENCE INTENSITY
TIME (s)
0
5
10
15
20
25
0
100
200
300
SILVER
QUARTZ
FLUORESCENCE INTENSITY
TIME (s)
0
4
8
12
16
20
24
0
100
200
300

FIG. 6

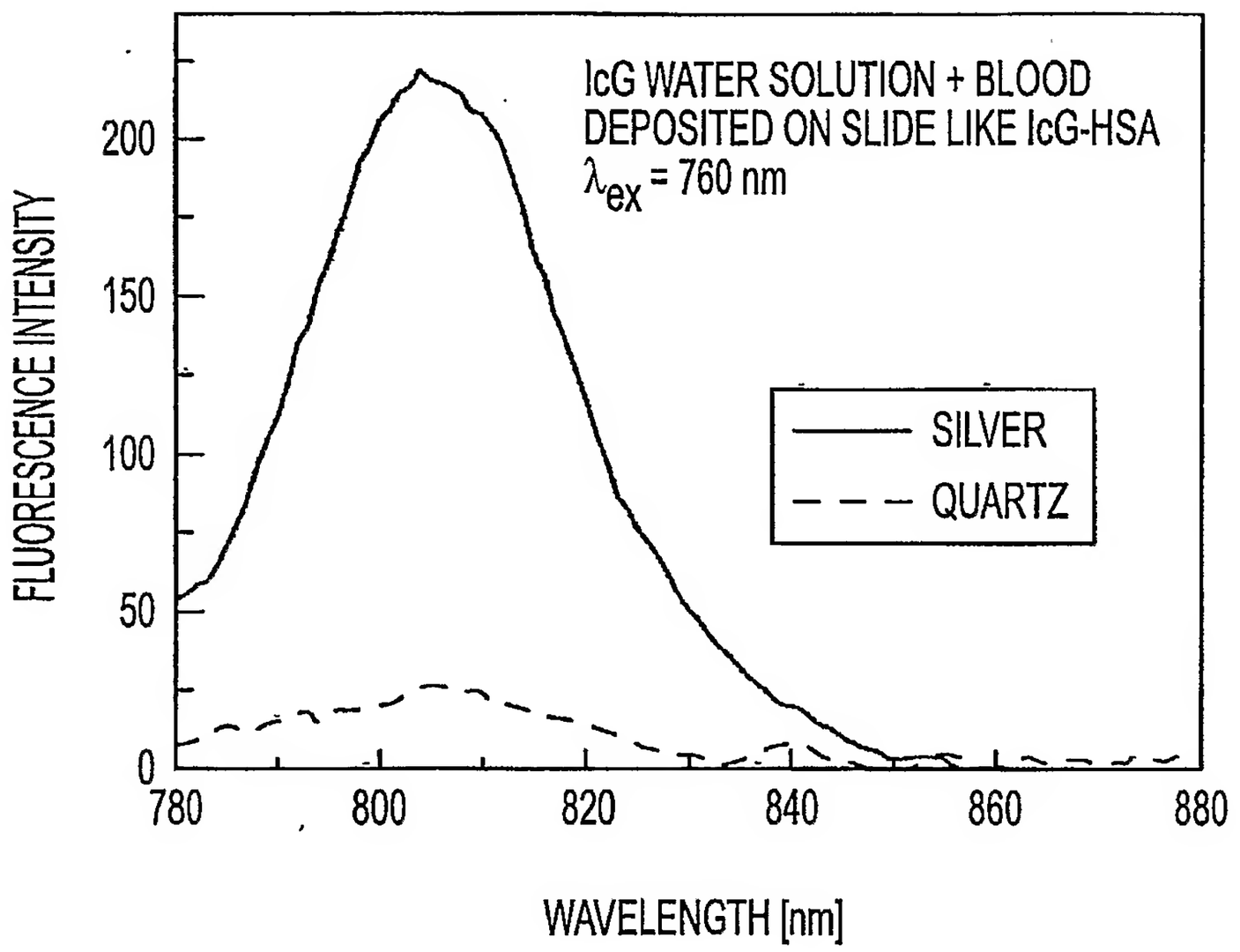
IcG WATER SOLUTION + BLOOD
DEPOSITED ON SLIDE LIKE IcG-HSA
λ_{ex} = 760 nm
SILVER
QUARTZ
FLUORESCENCE INTENSITY
0
50
100
150
200
780
800
820
840
860
880
WAVELENGTH [nm]

FIG. 7

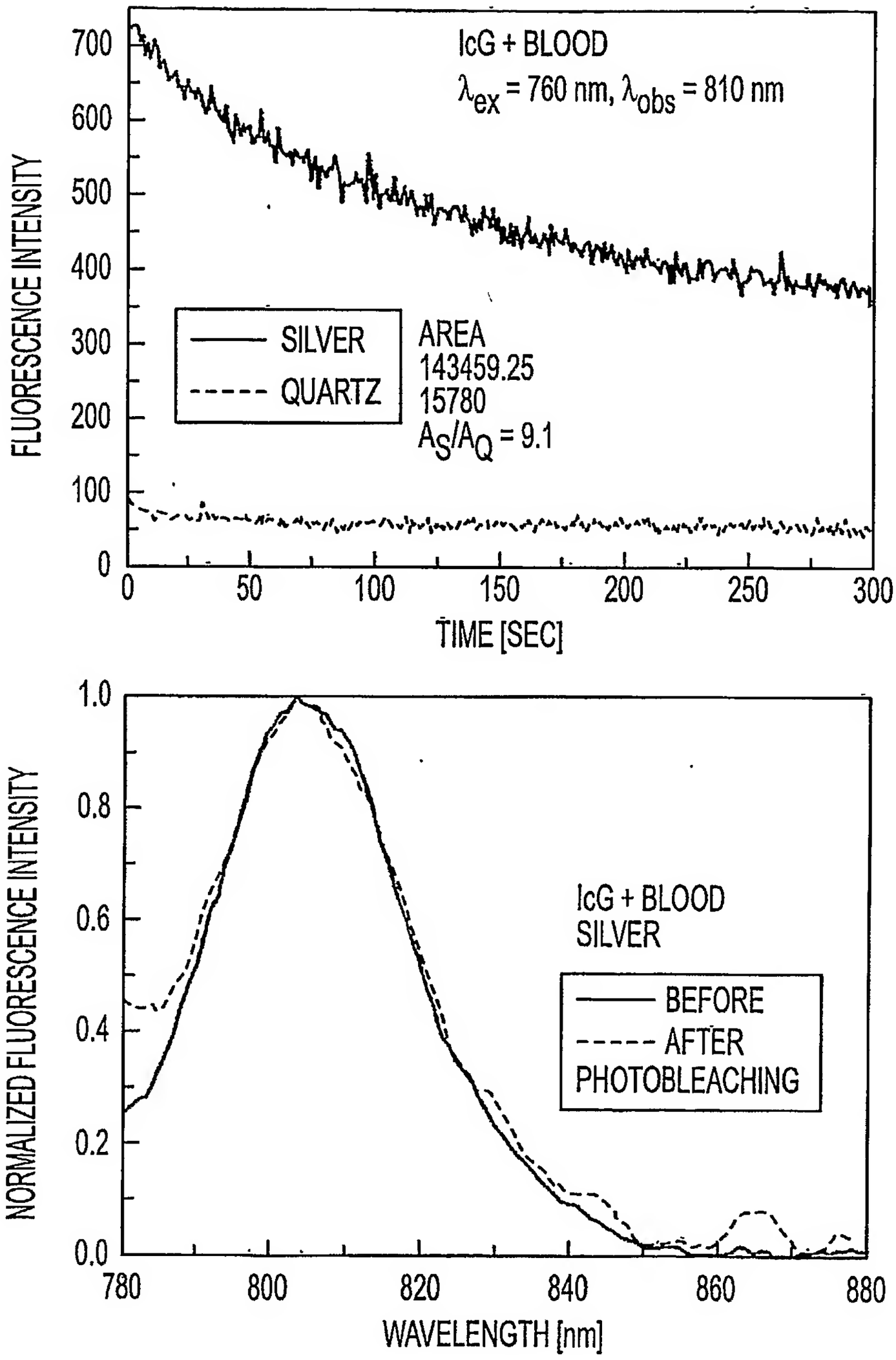
IcG + BLOOD
λ_{ex} = 760 nm, λ_{obs} = 810 nm
FLUORESCENCE INTENSITY
SILVER
QUARTZ
AREA
143459.25
15780
A_S/A_Q = 9.1
TIME [SEC]
NORMALIZED FLUORESCENCE INTENSITY
IcG + BLOOD
SILVER
BEFORE
AFTER PHOTOBLEACHING
WAVELENGTH [nm]

FIG. 8

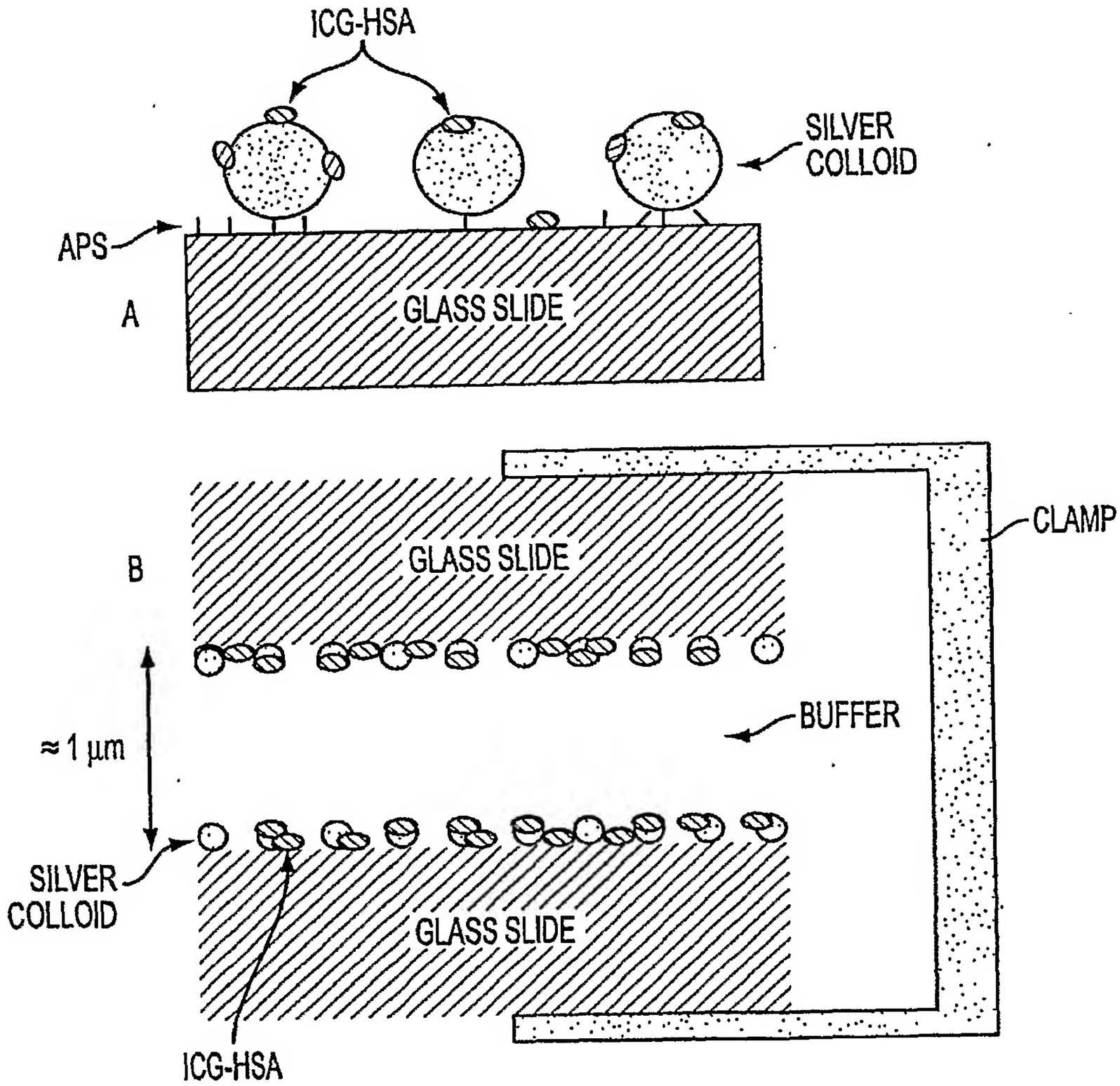
ICG-HSA
SILVER COLLOID
APS
A
GLASS SLIDE
B
GLASS SLIDE
CLAMP
BUFFER
≈ 1 µm
SILVER COLLOID
GLASS SLIDE
ICG-HSA

FIG. 9

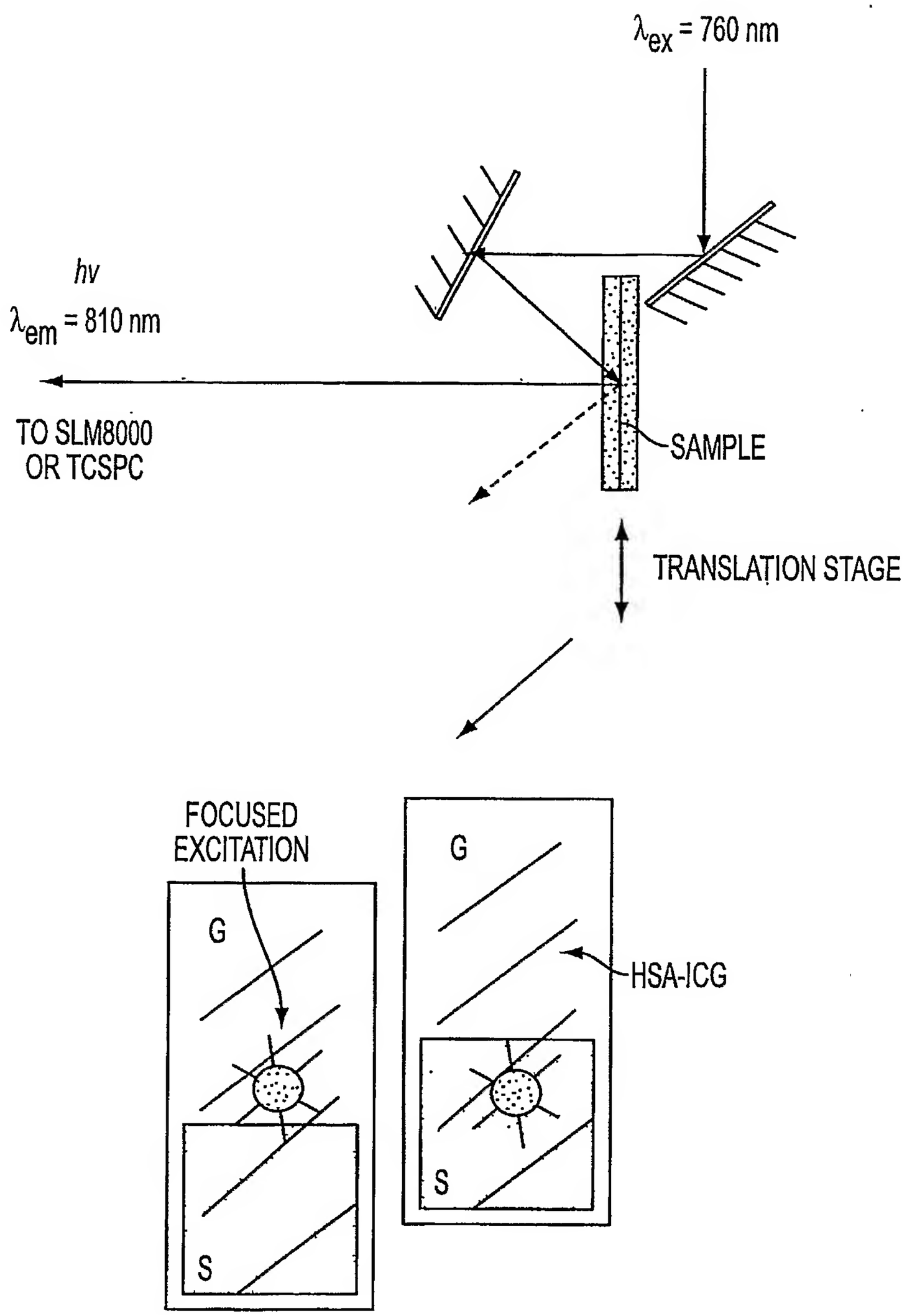
λ_{ex} = 760 nm
hv
λ_{em} = 810 nm
TO SLM8000
OR TCSPC
SAMPLE
TRANSLATION STAGE
FOCUSED
EXCITATION
G
S
G
S
HSA-ICG

FIG. 10

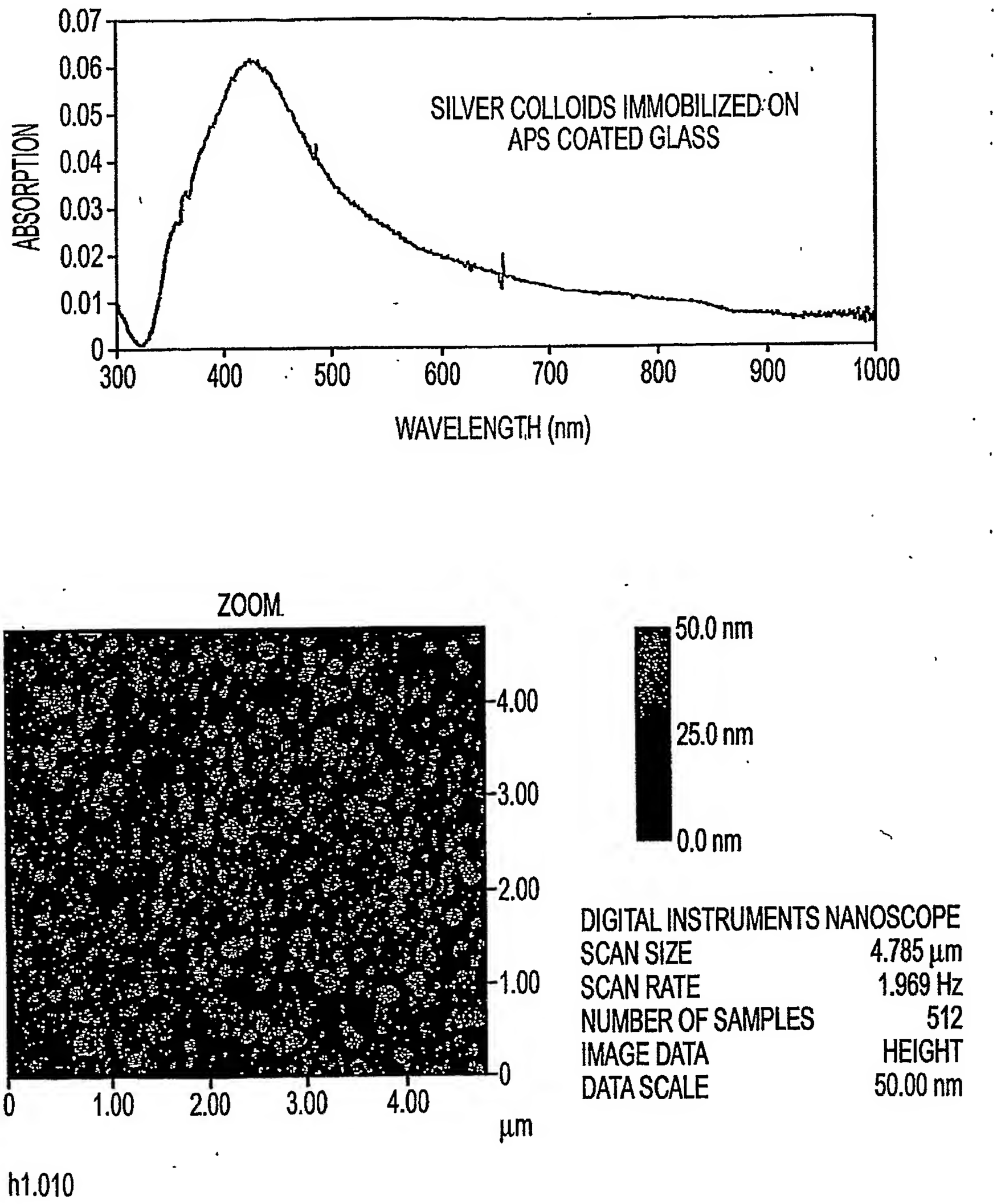
SILVER COLLOIDS IMMOBILIZED ON
APS COATED GLASS
ABSORPTION
0.07
0.06
0.05
0.04
0.03
0.02
0.01
0
300
400
500
600
700
800
900
1000
WAVELENGTH (nm)
ZOOM
4.00
3.00
2.00
1.00
0
0
1.00
2.00
3.00
4.00
µm
50.0 nm
25.0 nm
0.0 nm
DIGITAL INSTRUMENTS NANOSCOPE
SCAN SIZE 4.785 µm
SCAN RATE 1.969 Hz
NUMBER OF SAMPLES 512
IMAGE DATA HEIGHT
DATA SCALE 50.00 nm
h1.010

FIG. 11

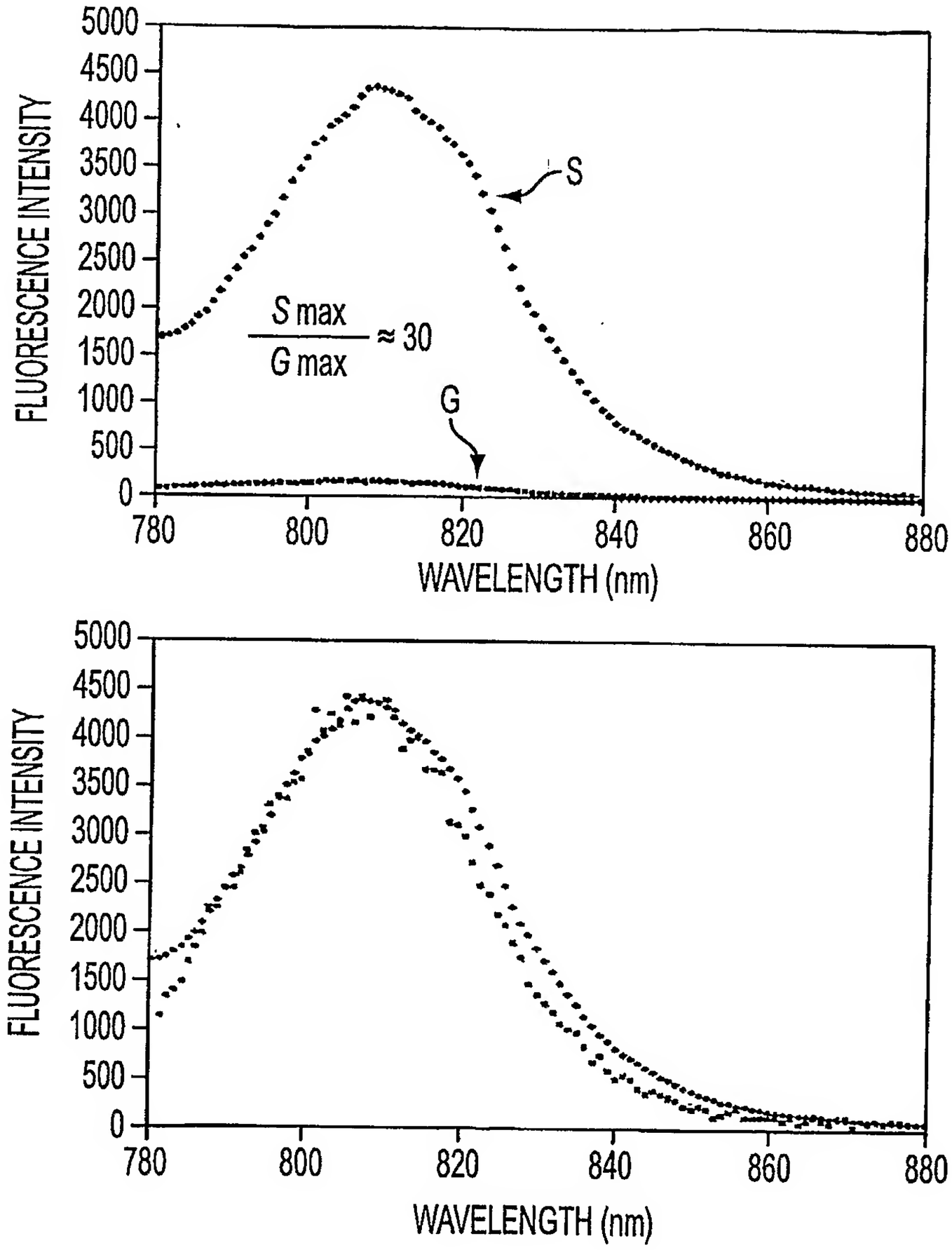
FLUORESCENCE INTENSITY
5000
4500
4000
3500
3000
2500
2000
1500
1000
500
0
780
800
820
840
860
880
WAVELENGTH (nm)
S
G
S max / G max ≈ 30

FIG. 12

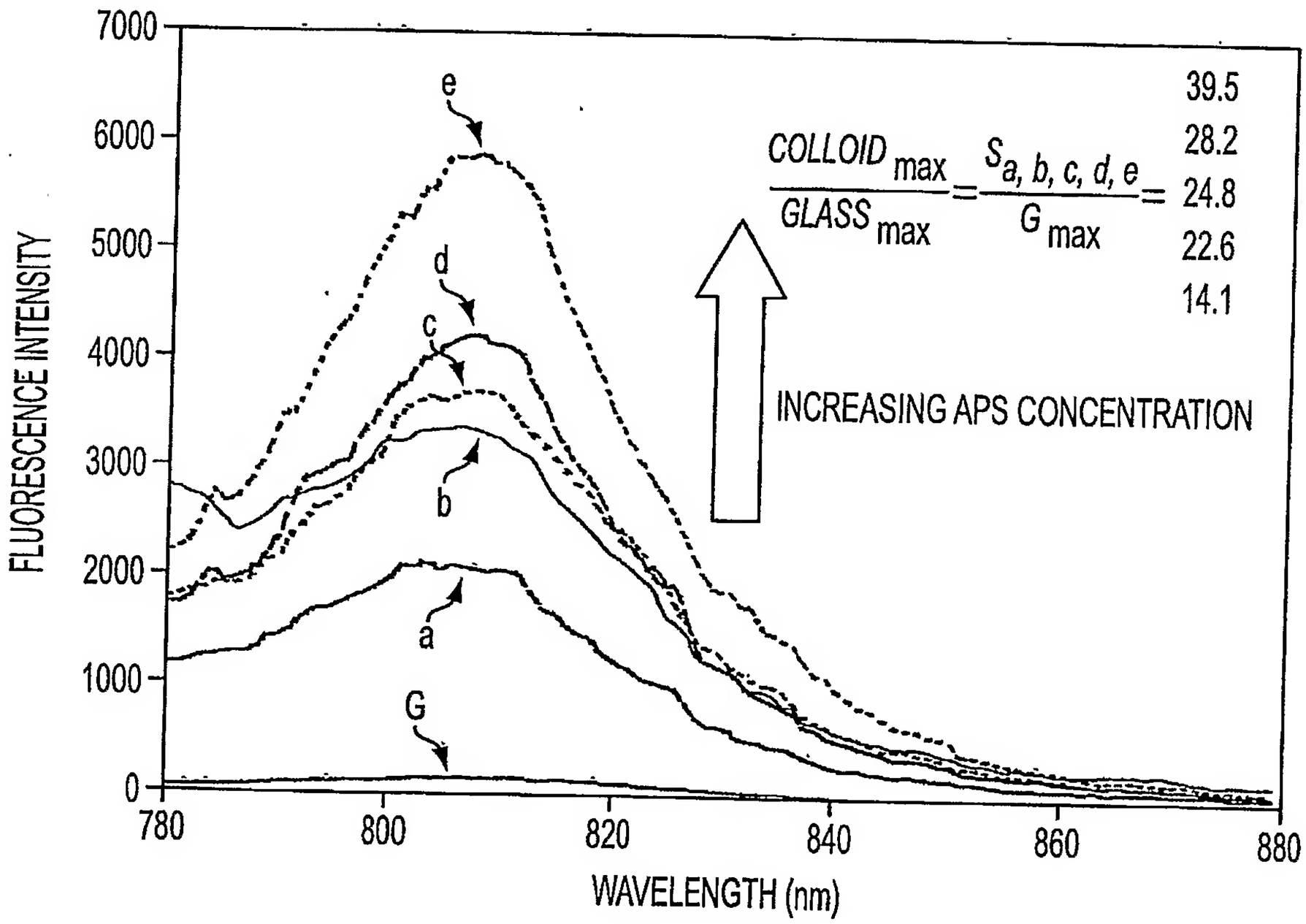
7000
6000
5000
4000
3000
2000
1000
0
780
800
820
840
860
880
FLUORESCENCE INTENSITY
WAVELENGTH (nm)
e
d
c
b
a
G
$\frac{COLLOID_{max}}{GLASS_{max}} = \frac{S_{a,b,c,d,e}}{G_{max}}$
39.5
28.2
24.8
22.6
14.1
INCREASING APS CONCENTRATION

FIG. 13

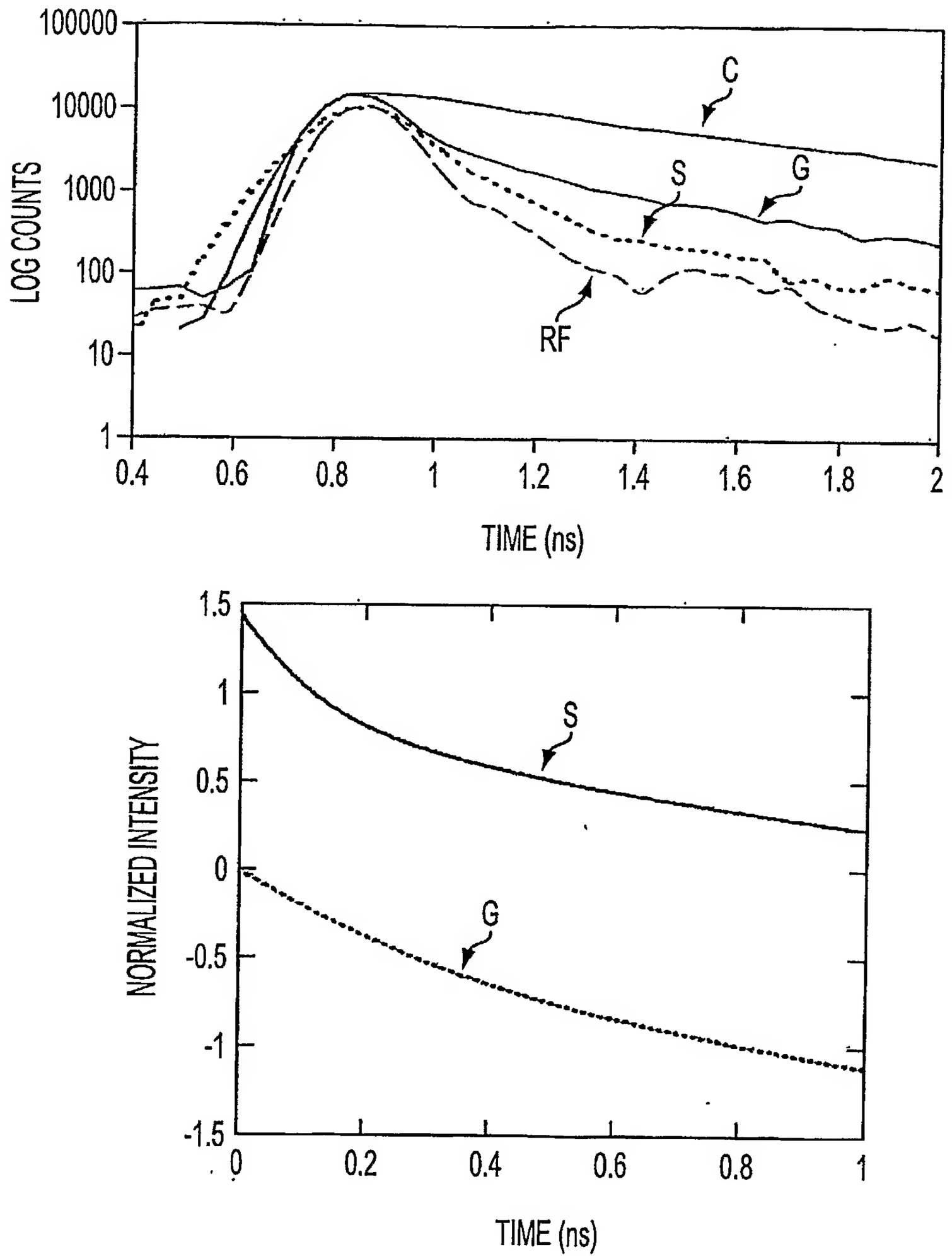
100000
10000
1000
100
10
1
LOG COUNTS
C
S
G
RF
0.4
0.6
0.8
1
1.2
1.4
1.6
1.8
2
TIME (ns)
1.5
1
0.5
0
-0.5
-1
-1.5
NORMALIZED INTENSITY
S
G
0
0.2
0.4
0.6
0.8
1
TIME (ns)

FIG. 14

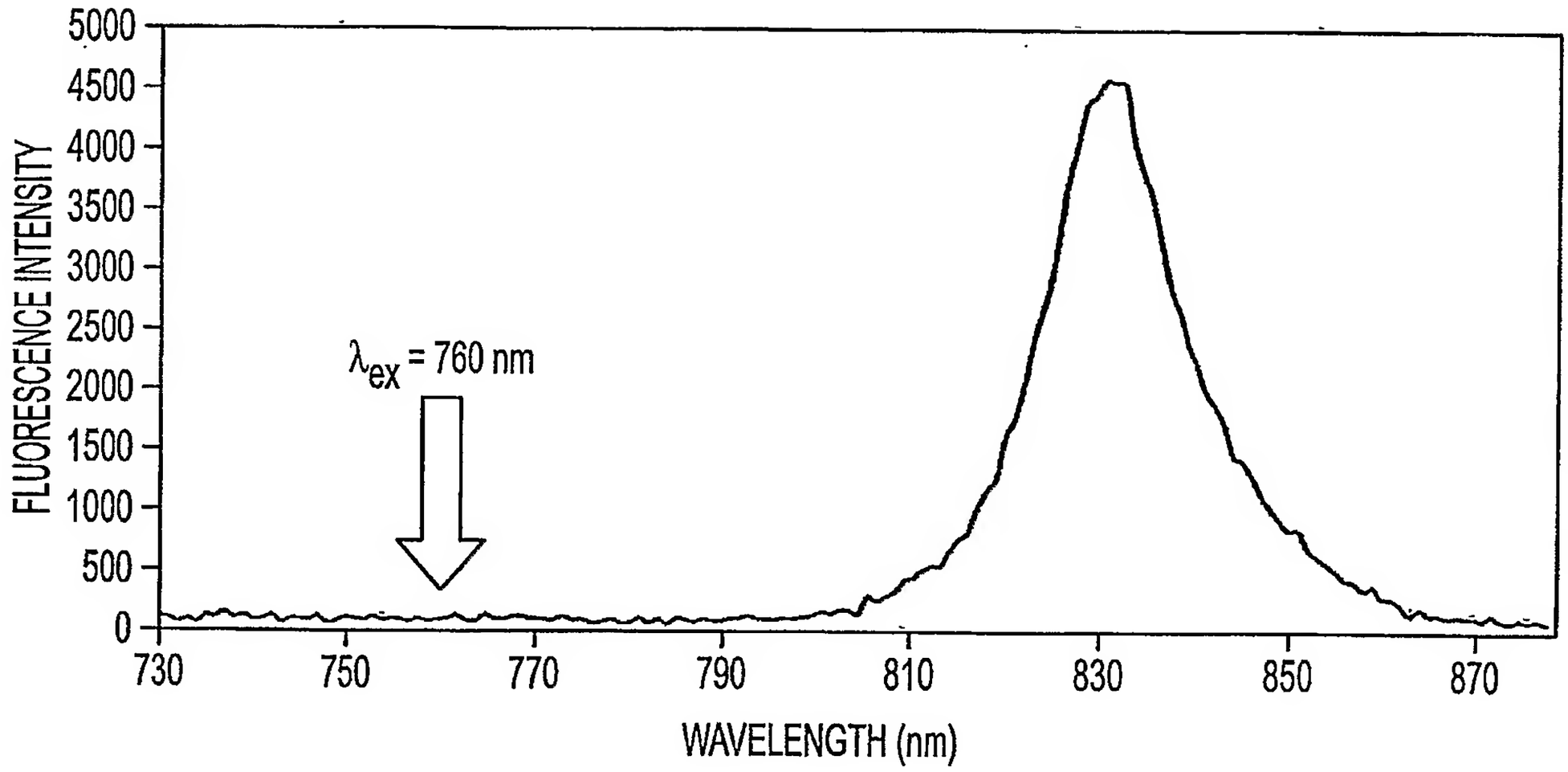
5000
4500
4000
3500
3000
2500
2000
1500
1000
500
0
FLUORESCENCE INTENSITY
λ_{ex} = 760 nm
730
750
770
790
810
830
850
870
WAVELENGTH (nm)

FIG. 15

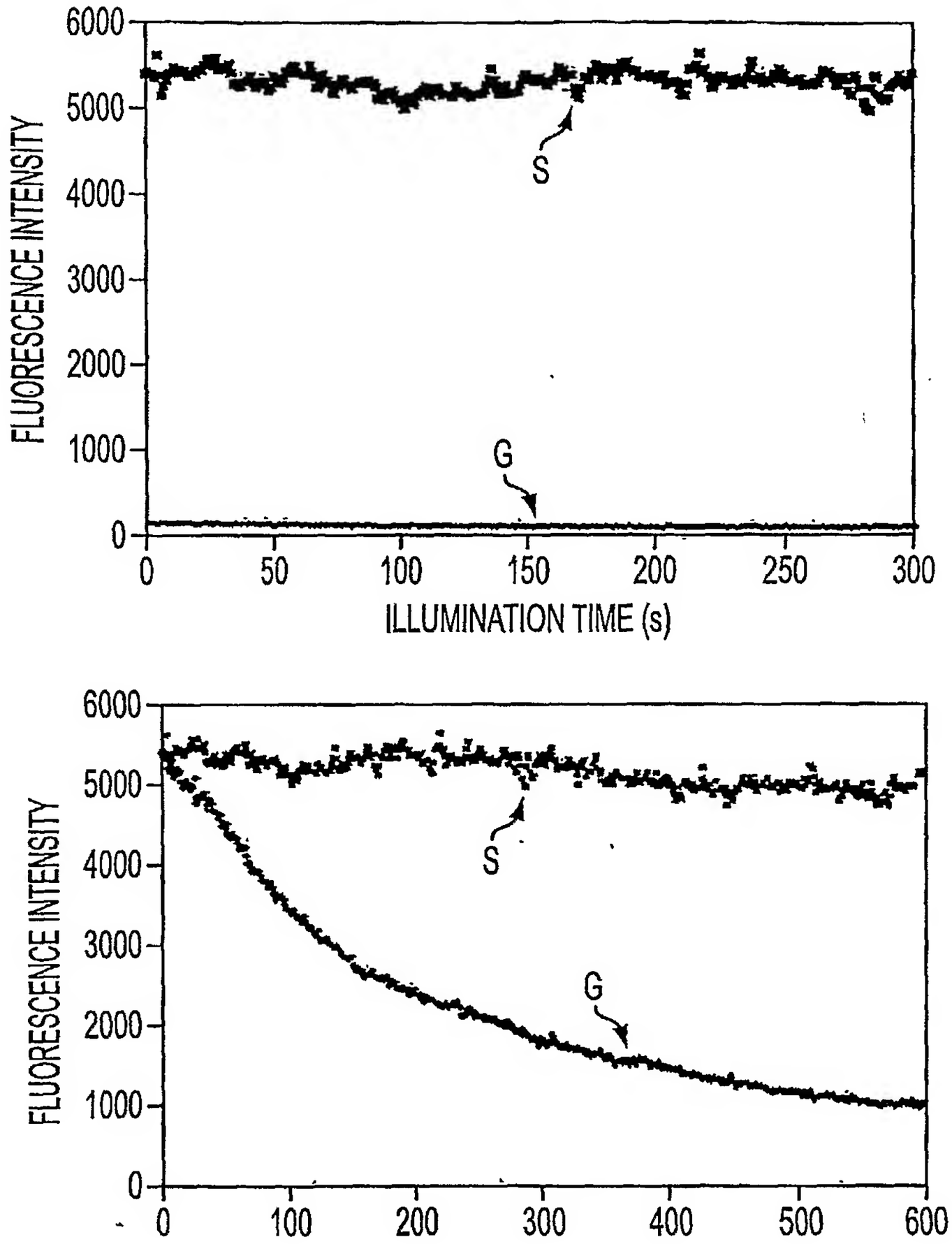
6000
5000
4000
3000
2000
1000
0
FLUORESCENCE INTENSITY
S
G
0
50
100
150
200
250
300
ILLUMINATION TIME (s)
6000
5000
4000
3000
2000
1000
0
FLUORESCENCE INTENSITY
S
G
0
100
200
300
400
500
600
ILLUMINATION TIME (s)

FIG. 16

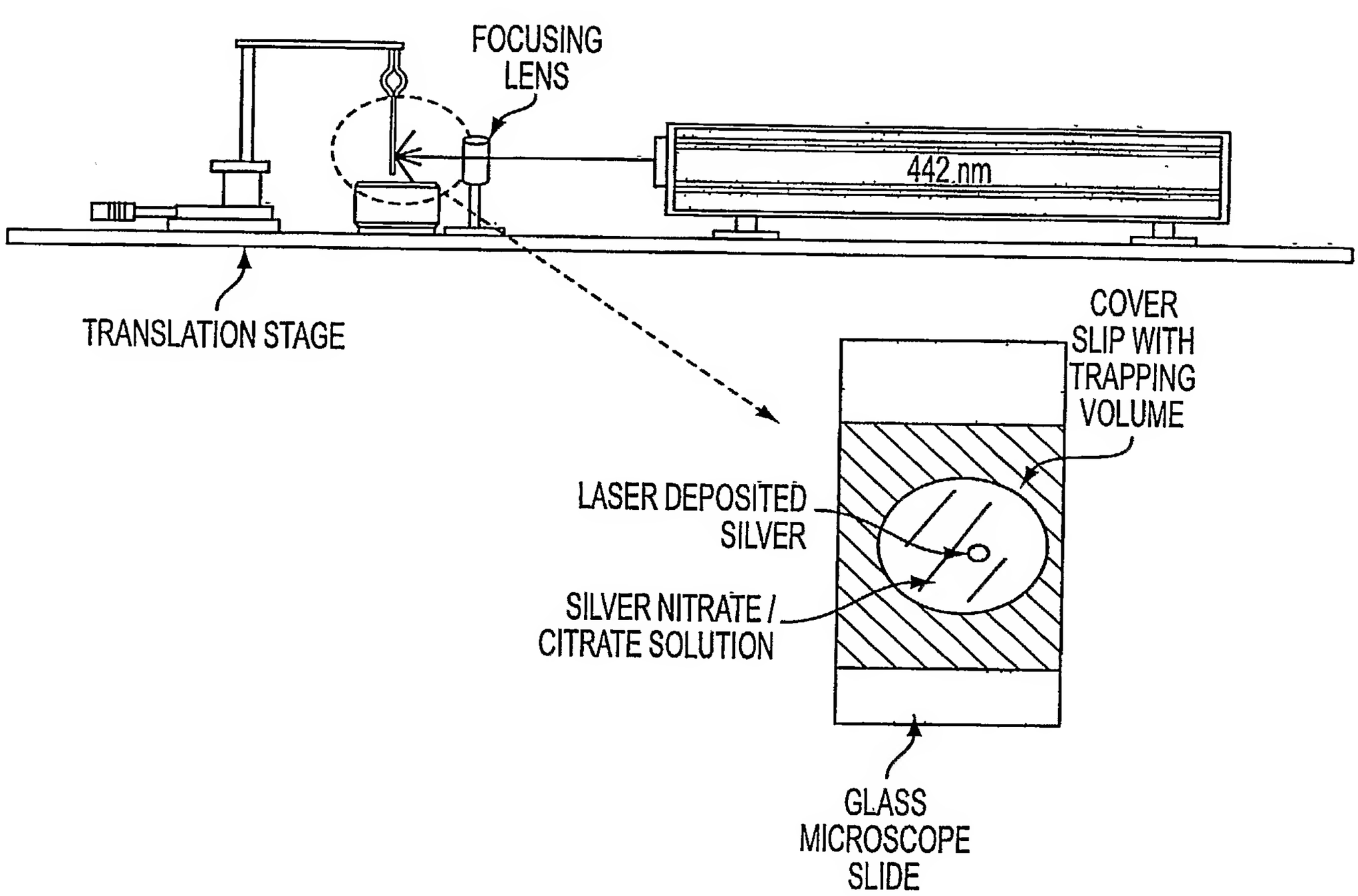
FOCUSING LENS
442 nm
TRANSLATION STAGE
COVER SLIP WITH TRAPPING VOLUME
LASER DEPOSITED SILVER
SILVER NITRATE / CITRATE SOLUTION
GLASS MICROSCOPE SLIDE

FIG. 17

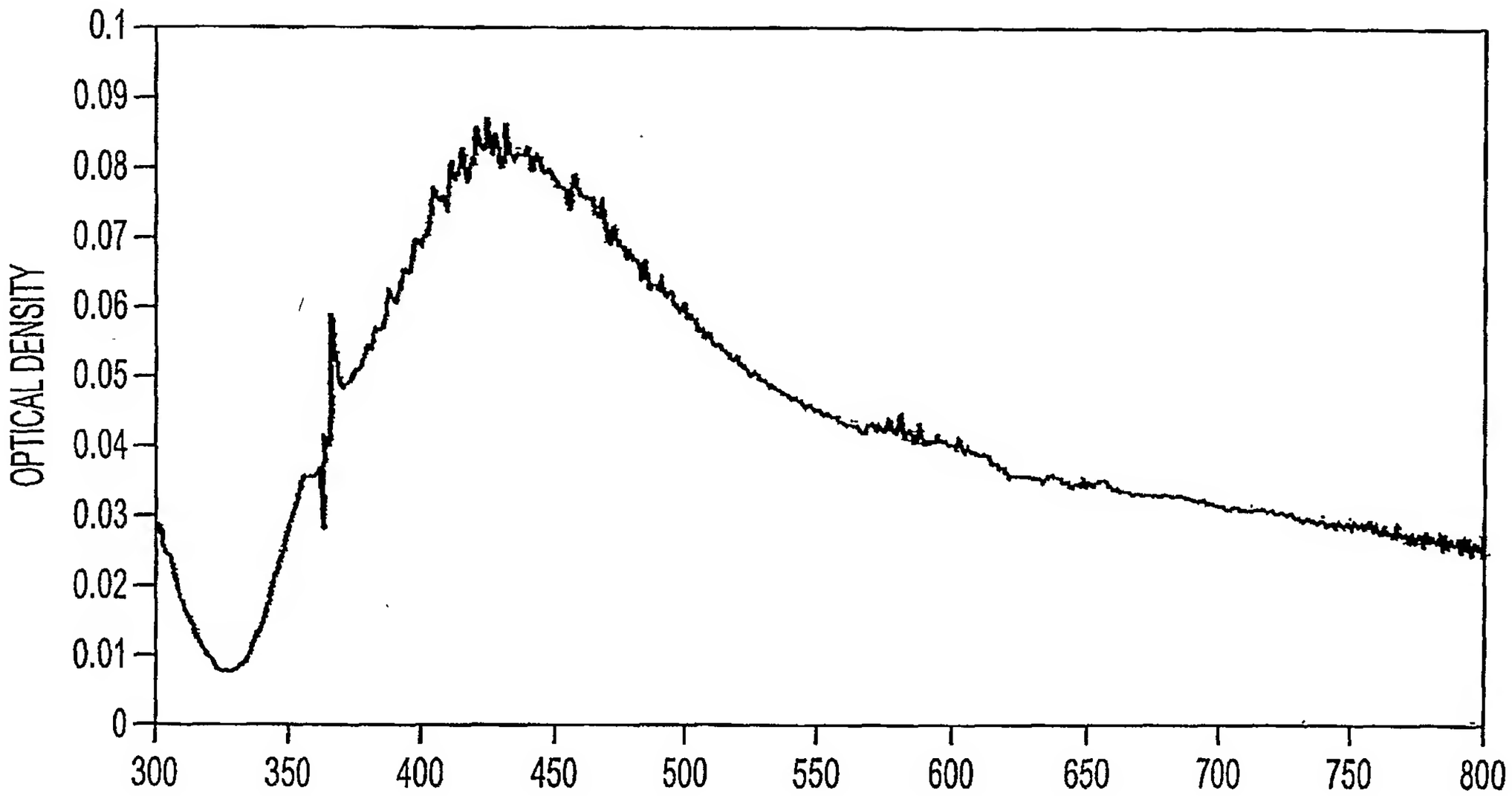
0.1
0.09
0.08
0.07
0.06
0.05
0.04
0.03
0.02
0.01
0
OPTICAL DENSITY
300
350
400
450
500
550
600
650
700
750
800
WAVELENGTH (nm)

FIG. 18

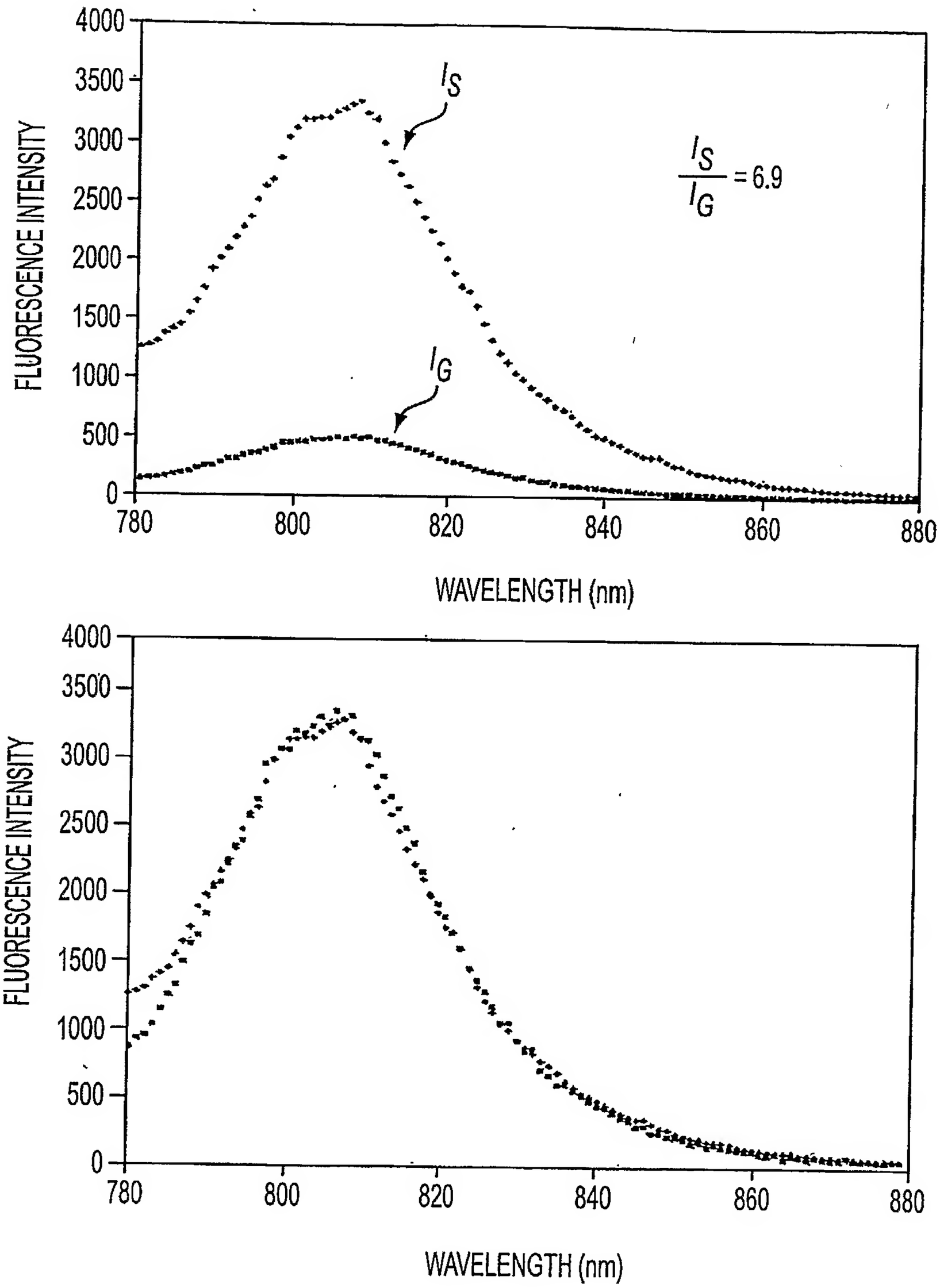
4000
3500
3000
2500
2000
1500
1000
500
0
FLUORESCENCE INTENSITY
780
800
820
840
860
880
WAVELENGTH (nm)
I_S
I_G
$\frac{I_S}{I_G} = 6.9$

FIG. 19

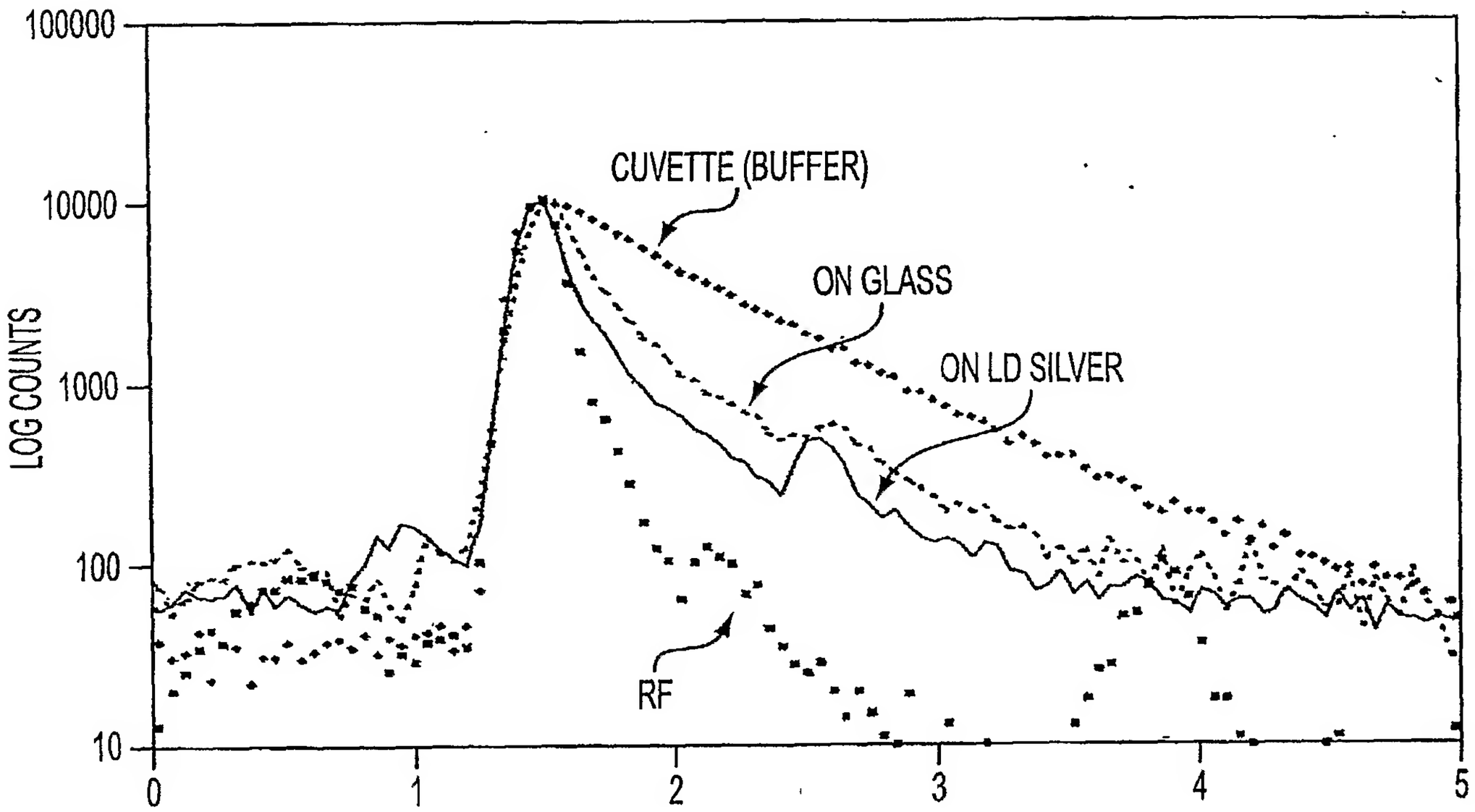
100000
10000
1000
100
10
LOG COUNTS
CUVETTE (BUFFER)
ON GLASS
ON LD SILVER
RF
0
1
2
3
4
5
TIME (ns)

FIG. 20

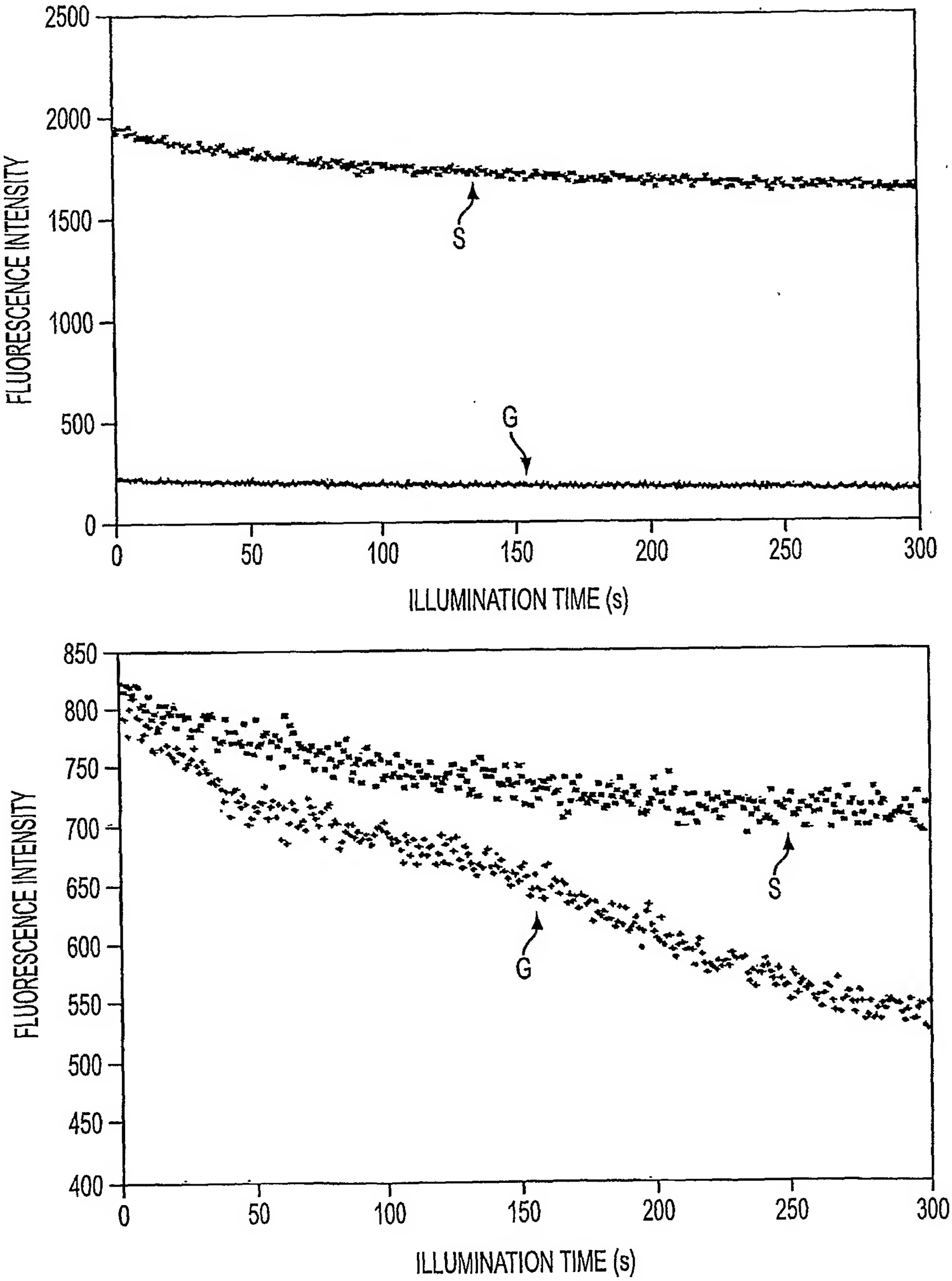
2500
2000
1500
1000
500
0
FLUORESCENCE INTENSITY
S
G
0
50
100
150
200
250
300
ILLUMINATION TIME (s)
850
800
750
700
650
600
550
500
450
400
FLUORESCENCE INTENSITY
S
G
0
50
100
150
200
250
300
ILLUMINATION TIME (s)

FIG. 21

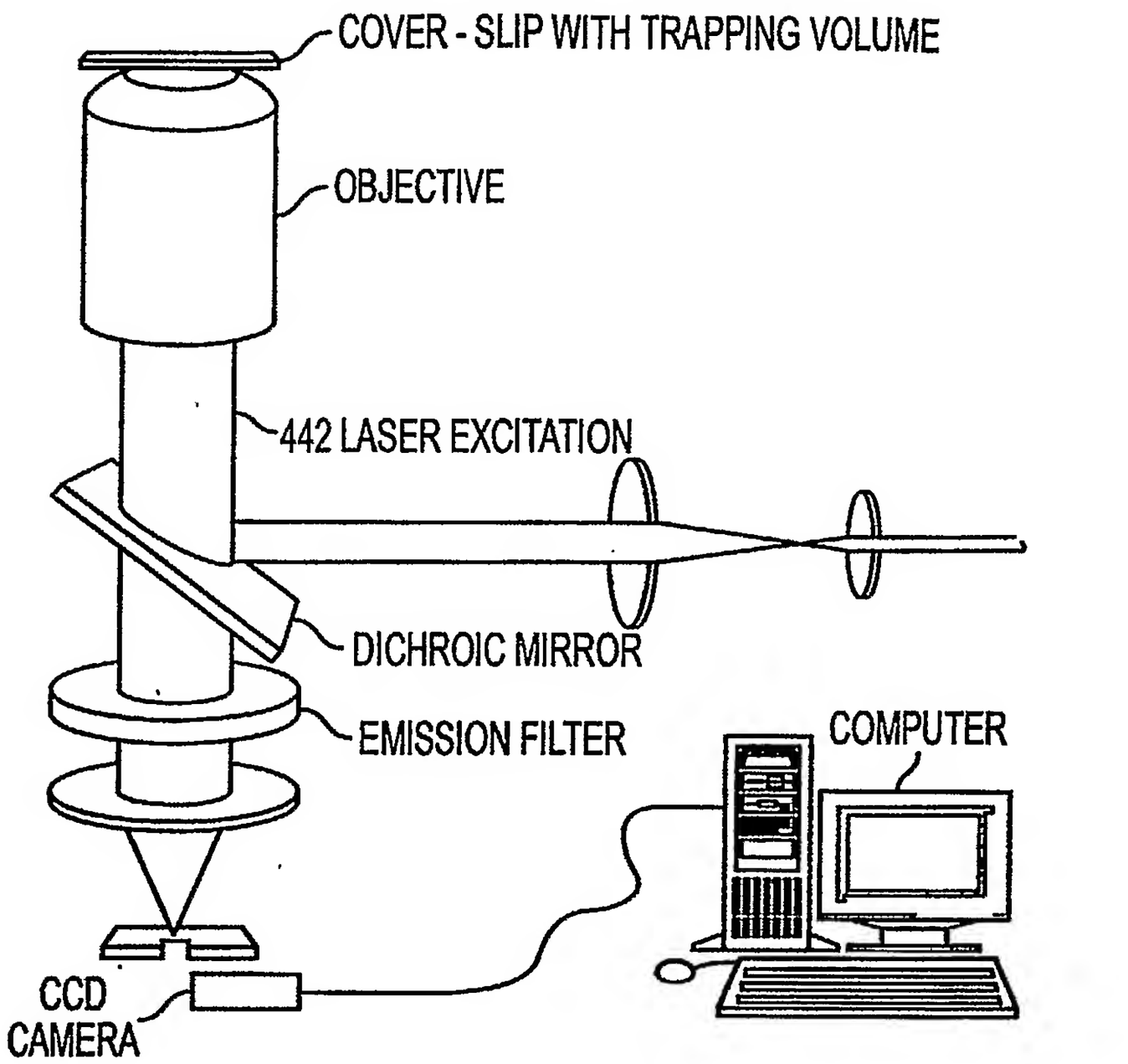
COVER - SLIP WITH TRAPPING VOLUME
OBJECTIVE
442 LASER EXCITATION
DICHROIC MIRROR
EMISSION FILTER
COMPUTER
CCD CAMERA

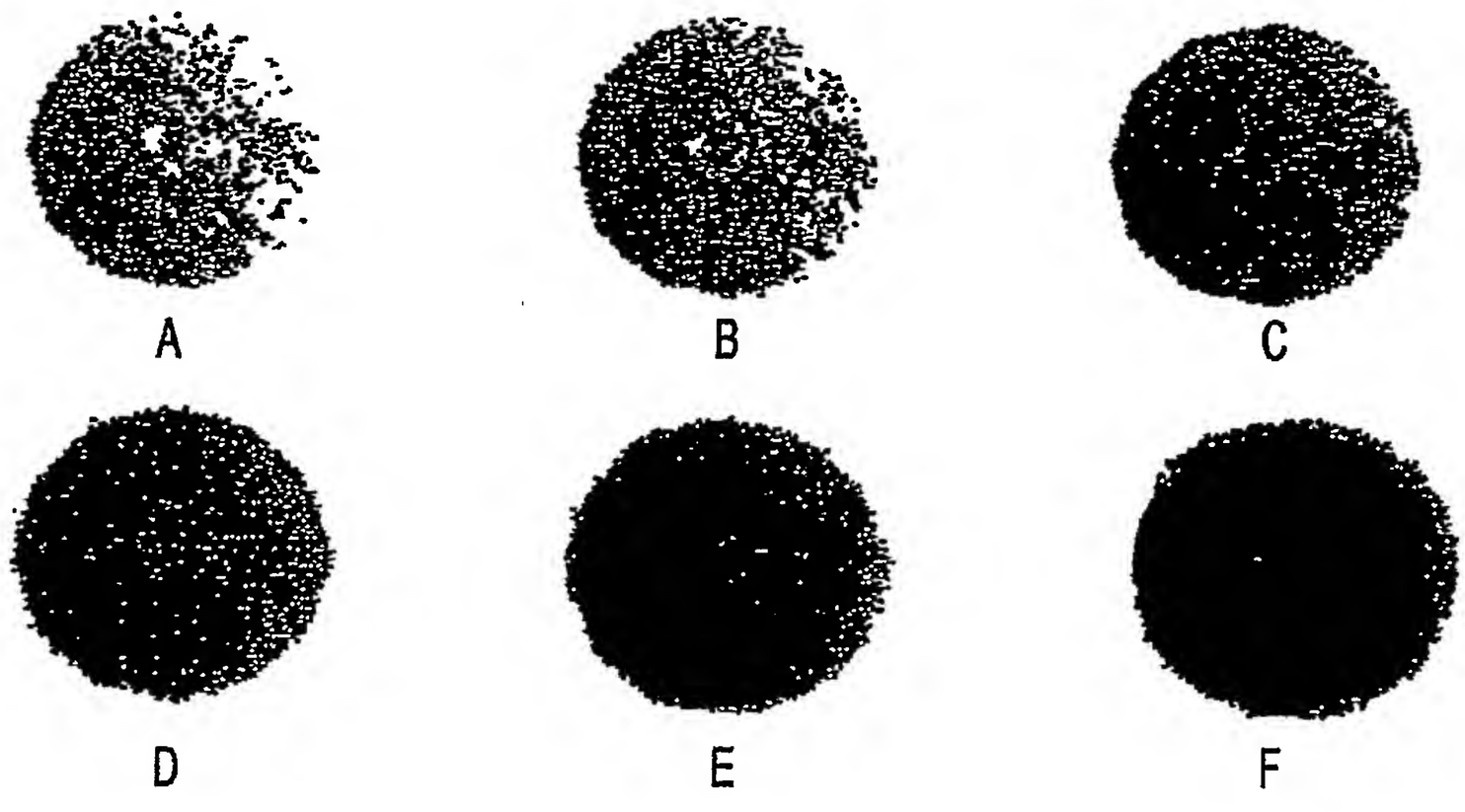
A
B
C
D
E
F

FIG. 22